MICROBIOLOGY AND MOLECULAR BIOLOGY REVIEWS, Dec. 2007, p. 600–619 Vol. 71, No. 4
1092-2172/07/$08.00+0 doi:10.1128/MMBR.00011-07

The Autodisplay Story, from Discovery to Biotechnical and Biomedical Applications

Joachim Jose[1] and Thomas F. Meyer[2]*

Bioanalytics, Institute of Pharmaceutical and Medicinal Chemistry, Heinrich-Heine-University, Universitätsstr. 1, D-40225 Düsseldorf,[1] and Department of Molecular Biology, Max Planck Institute for Infection Biology, Charitéplatz 1, D-10117 Berlin,[2] Germany

INTRODUCTION

The display of a protein or peptide with a distinct function at the cellular surface bears considerable advantages for many biotechnical applications (67, 143). The molecule displayed at the cell surface is freely accessible to the substrate or binding partner in activity or binding studies. Proteins have proven to be more stable when connected to a matrix rather than as free molecules. In this case, the cell envelope acts as a matrix. Displaying proteins on the cell surface also makes preparing or purifying the protein unnecessary in many instances. Whole cells displaying the molecule of interest can be used in reactions or analytical assays and then can be simply removed by centrifugation. Bacterial surface display exhibits another significant advantage during the creation and screening of peptide or protein libraries. The gene corresponding to the protein or peptide displayed on the cell surface is coselected and can easily be cloned for rapid sequence determination, initial structural predictions, and various other studies and applications (45). Phage display systems had been developed for similar reasons in the mid-1980s. Phage display allows the expression of peptides and small proteins in the envelope of the filamentous bacteriophage via fusion with the pIII coat protein (115, 116). Live-cell surface display, however, offers additional advantages over phage display. Bacteria replicate autonomously, in contrast to bacteriophages, and are sufficiently large to be analyzed by optical methods, including fluorescence microscopy, or high-throughput methods, such as fluorescence-activated cell sorting (FACS) (13, 20, 21, 24, 46, 52, 142). Since the first reports of bacterial display of heterologous proteins in 1986 by Freudl and coworkers (26) and Charbit and coworkers (17), an extraordinary number of different display systems has been established for yeasts (15, 106, 129, 132, 149), gram-positive bacteria (40, 69, 84, 102, 117, 119, 123), and gram-negative bacteria (1, 25, 27, 53, 56, 59, 63, 71, 72, 112, 118, 141). These systems have been employed for a wide range of biotechnical and biomedical applications and have prompted substantial progress in whole-cell biocatalysis, live vaccine development, biosorbent and biosensor development, epitope mapping, antigen delivery, inhibitor design, and protein/peptide library screening (for overviews, see references 5, 28, 67, and 143).

A universal display system must have a number of crucial features. It should pose minimal restrictions on the size and structure of the protein to be displayed. The system should utilize standard protocols in molecular biology and standard bacterial strains. Tools must also be available to analyze and evaluate the efficiency of passenger display. Optimally, the system should be simple and easy to handle to minimize unexpected obstacles. The autodisplay system has been developed to fulfill these requirements to the greatest possible extent (73). In this review, we summarize the basic structural features and the advantages of this *Escherichia coli* surface display system and give examples for its successful application

* Corresponding author. Mailing address: Department of Molecular Biology, Max Planck Institute for Infection Biology, Charitéplatz 1, D-10117 Berlin, Germany. Phone: 49/30-28460-400. Fax: 49/30-28460-401. E-mail: tfm@mpiib-berlin.mpg.de.

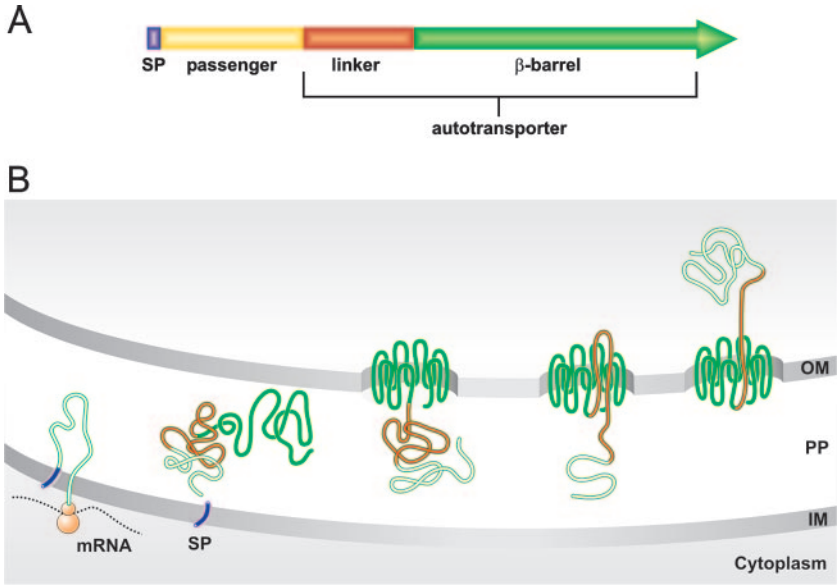

FIG. 1. Secretion mechanism of the autotransporter proteins. (A) Structure of the polyprotein precursor. (B) Transport of the recombinant passenger. By the use of a typical signal peptide, a precursor protein is transported across the inner membrane. After arrival at the periplasm, the C-terminal part of the precursor folds as a porin-like structure, a so-called β-barrel within the outer membrane, and the passenger is transmitted to the cell surface. SP, signal peptide; IM, inner membrane; PP, periplasm; OM, outer membrane.

in enzyme display, whole-cell biocatalysis, inhibitor display and design, library screening, and live vaccine development.

IgA1 PROTEASE

IgA1 Protease from *Neisseria gonorrhoeae*: Discovery of the First Autotransporter and Initial Applications

The autodisplay system was developed based on the secretion mechanism of the autotransporter family of proteins (37, 48, 70). Gram-negative bacteria have evolved the autotransporter pathway to transport proteins to the cell surface or secrete proteins into the extracellular milieu. This system is outstanding in its apparent simplicity. The autotransporters are synthesized as multidomain proteins containing the structural requirements sufficient for transport to the cell surface. The immunoglobulin A1 (IgA1) protease of *Neisseria gonorrhoeae* was the first family member to be discovered and was characterized in the late 1980s (35, 77, 92). A hypothetical model was proposed for its mechanism of secretion (Fig. 1). Briefly, a typical signal peptide aids the transport of the precursor across the inner membrane. Upon arrival in the periplasm, the C-terminal part of the precursor forms a porin-like structure, termed the β-barrel, within the outer membrane. The N-terminally attached passenger, which in this case is the actual protease linked to two additional peptides, is translocated to the cell surface through this pore. A linker peptide between the β-barrel and the passenger is required to achieve full surface exposure and functionality of the passenger protein (Fig. 1) (55, 73). Translocation across the outer membrane, in particular, has been subject of controversial discussion for some time (136, 138). Recent mechanistic studies (52, 66, 81, 101) and the first crystal structure reported for the translocation unit of an autotransporter protein (87) support the originally proposed concept. Nevertheless, several other investigators have implicated Omp85, a highly conserved bacterial protein present in a wide variety of different species, as having a role in the secretion of autotransporter proteins and have proposed the translocation of folded domains which contradict the original model (97, 128, 133, 136).

Autotransporter proteins are currently assigned to the type V protein secretion system. The type V secretion system can be subdivided into type Va or IgA1 protease-type autotransporters (AT-1 pathway), type Vb or two-partner secretion pathway, and type Vc (AT-2 pathway). On the basis of structural and functional criteria, as well as phylogenetic analysis of their C-terminal translocating domains, autotransporters can be divided into 11 clusters (38). For the type Vb pathway, the passenger domain and the β-barrel-forming domain that translocates the passenger domain across the outer membrane are produced as two separate proteins, TpsA and TpsB, each bearing their own signal peptides for inner membrane transport (41). In the type Vc pathway, the outer membrane translocation unit depends on trimerization, where the C-terminal parts of each monomer contribute four β-strands to assemble the complete pore (76). With the exception of HiaI, an adhesin from *Haemophilus influenzae*, which was used for the surface display of PhoA and a domain of Hap (122), none of the type Vb or Vc members have been used to date to transport recombinant proteins or to display recombinant proteins on the cell surface. Even though the intricacies of type Va autotransporter secretion as well as their structural and functional needs remain unclear, it was realized at an early stage that this secretion mechanism could be exploited in *E. coli* for the transport of a recombinant protein. The coding region for the endogenous passenger need only be replaced by the coding region for the recombinant protein of interest and subsequently expressed in *E. coli* (Fig. 2) (56). Proof of principle was demonstrated by several examples of recombinant polypep-

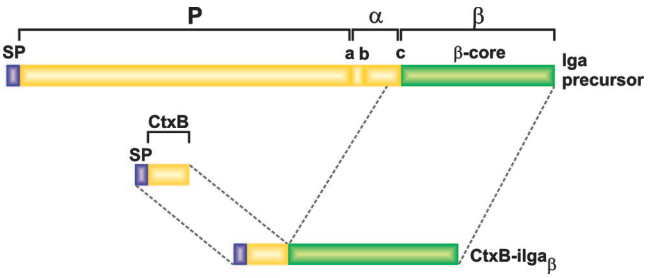

FIG. 2. Linear structure of the CTB-IgA$_\beta$ hybrid protein, used for the first surface display of a recombinant protein with the aid of an autotransporter. SP, signal peptide; P, passenger.

tides (58, 93), but extensive biotechnical applications failed to appear. In particular, limitations of the secretory performance of the *Neisseria* protein in the heterologous *E. coli* host background prevented the biotechnical exploitation of this system.

Some general considerations about the surface display of recombinant proteins using autotransporters must be stressed at this point. It is sensible to use *E. coli* as a gram-negative host organism for the surface display of recombinant proteins, since the metabolism and genetic repertoire of *E. coli* have been thoroughly investigated. A wide variety of tools are also available, including plasmids and other vectors, mutant strains, and methods for DNA transfer, DNA isolation, and mutagenesis. Attenuated strains of the closely related genus *Salmonella* can also be used for oral vaccination approaches. As some of the genetic engineering tools established for *E. coli* are transferable to a variety of enterobacterial strains, it was reasonable to use the *Neisseria* IgA1 protease as the prototype autotransporter for surface display of a recombinant passenger in both *E. coli* and *Salmonella* hosts. As a consequence, not only the passenger but also the transporter protein were heterologous and foreign to the host organism species. The β-subunit of cholera toxin (CTB, former CtxB) was used a passenger in these initial experiments (Fig. 2). Important information about the basic principles of autotransporter secretion was gathered in these initial experiments. The passenger must be in an unfolded state for surface translocation (56). The formation of disulfide bonds in the periplasm blocks protein transport (49, 56). The role of the host-derived outer membrane protease T, OmpT, in the extracellular release of passengers (58) and the dimensions and structural and functional features of the β-barrel outer membrane translocation unit (55) were defined. All subsequently discovered autotransporter proteins of type Va were structurally similar to the prototype of the family, the IgA1 protease. These proteins are comprised of a signal peptide at the N terminus followed by the passenger domain(s), a linker, and the β-barrel domain. These initial experiments were essential in guiding subsequent investigations of the autotransporter mechanisms. However, the genetic setting of these initial experiments was not fully conducive to the development of biotechnical applications. The bacterial cells used in these early experiments were grown on solid media (agar plates), which is acceptable for basic research but cumbersome for most biotechnical applications. Early attempts using liquid media were unsuccessful. This limitation may only have been due to using the heterologous *Neisseria* transporters within the *E. coli* host background rather than the passenger CTB, as was later suggested (142). In these experiments, the translocation unit of the IgA1 protease was used to display a library of *Ecballium elaterium* trypsin inhibitor (EETI-II) variants on the surface of *E. coli* cells in order to study trypsin binding and folding of the peptide inhibitor. The positive variants were sorted by FACS but were unable to replicate. The sequence of the trypsin inhibitor variants had to be obtained using PCR amplification of the variant DNA.

The view that this was a host-specific phenomenon, rather than due to the recombinant passenger transported, was supported recently by investigations of the role of Omp85 in the assembly of β-barrel proteins within the outer membrane. It was demonstrated by Robert et al. (97) that the Omp85 assembly factor recognized its outer membrane protein substrates by virtue of their C-terminal signature sequences. This interaction was shown to be species specific, which is reflected by a consensus C-terminal motif identified in the outer membrane proteins of *E. coli* that differs from the corresponding motif in *Neisseria*. It could explain the inefficient assembly of *Neisseria* outer membrane proteins, and hence deficiencies of the *E. coli* autotransporter proteins, on a molecular level. Supplying the neisserial PorA with the *E. coli* C-terminal motif clearly demonstrated the impact of this observation, enabling the proper assembly of a *Neisseria* β-barrel protein in the recombinant *E. coli* host. Ref.

Biotechnical and Biomedical Applications of IgA1 Protease-Mediated Surface Display

Despite the obstacles of heterologous protein expression in *E. coli*, the *Neisseria* autotransporter has been utilized in many cases by de Lorenzo and coworkers for the surface display of heterologous passengers. This included single-chain Fv (scFv) antibody fragments (135–137), a mouse metallothionein (MT) (130, 131), and the Fos and the Jun leucine zipper domains (135), as well as the E-tag and a polyhistidine tag (138, 135, 137). One major insight gained from these investigations is that recombinant proteins displayed on the *E. coli* cell surface by the IgA1 protease translocation unit can adapt an active, functional conformation. Cells displaying different scFv fragments were used for antigen binding studies using a whole cell enzyme-linked immunosorbent assay (ELISA) and to neutralize the transmissible gastroenteritis coronavirus as an infectious agent in epithelial cell cultures. The latter finding especially has paved the way for the application of this *E. coli* type in an antiviral strategy within its natural environment, the intestine.

A promising biotechnical application was achieved by the surface display of the mouse MT protein using the IgA1 protease translocation unit. MTs are small cysteine-rich proteins that bind heavy metals and are produced by mice and other eukaryotic organisms. In addition to *E. coli*, *Ralstonia eutropha* (formerly *Alcaligenes eutrophus*) was chosen as a host organism, since its natural habitat is soil and the chances for survival in that environment are much better for this organism than for *E. coli*. Moreover, *R. eutropha* has a natural resistance to heavy metals. This resistance is mediated by a proton-driven heavy metal efflux pump. The cation/proton antiport, i.e., heavy metal efflux and proton uptake, leads to an increase in the pH in the vicinity of the cell and subsequently to the precipitation of

heavy metal carbonates. Cells of *R. eutropha* displaying the mouse MT were used to collect Cd^{2+} ions from liquid media as well as for the detoxification of polluted soil. It was shown that soil contaminated with 150 μM cadmium salts strongly decreased plant growth of *Nicotiana bentamiana*, but after inoculation of the soil with *R. eutropha* cells displaying the MT protein, this negative effect on plant growth was countermanded (130). Further improvements are required before cells displaying MTs can be used for bioremediation of soil contaminated with cadmium; however, two important observations can be derived from this pioneering work. First, cell engineering protocols developed for *E. coli* for the surface display of recombinant proteins can be transferred to other species, including those having their natural habitat in extreme environments. Second, the IgA1 protease translocation unit is heterologously applicable, since it was demonstrated that the surface display of MT was possible not only in *E. coli* and *R. eutropha* (130) but also in *Pseudomonas putida* (131), another natural soil inhabitant. This supports the original idea proposed after expressing the *Neisseria* IgA1 protease polyprotein precursor in *E. coli* (35, 92) and later in *Salmonella* (56), i.e., that this transport mechanism was the paradigm for all gram-negative bacteria. Transport of the protein was facilitated by simply transferring the precursor protein gene from the natural to the heterologous host. The precursor contains sufficient structural information for surface translocation, and no cofactors are required. More recent investigations appear to indicate the involvement of additional proteins or chaperones in the autotransporter secretion pathway (86, 126, 133). Taking these results together, the initial conclusion could be modified to say that any additional proteins or cofactors required for autotransporter-mediated surface display of passenger proteins can be provided at least by a variety of different species if not by all gram-negative bacteria. Autotransporter proteins can be considered to be distributed ubiquitously throughout all genera of the *Alpha-*, *Beta-*, *Gamma-*, and *Epsilonproteobacteria* and in the phylum *Chlamydia*.

The fusion protein constructs consisting of recombinant passenger proteins and the IgA1 protease translocation unit were also used for investigations on the mechanism of surface translocation in *E. coli*. It was found that the purified translocation unit formed a ring-like oligomeric complex consisting of at least six monomers in the outer membrane with a central cavity of about 2 nm in diameter (138). It was hypothesized that the transport of the passenger domain to the cell surface proceeds through this oligomeric ring shaped by the translocation unit monomers. This hypothesis made autotransporter translocation to the cell surface similar to the mechanism proposed previously for fimbrial ushers or secretins (127) and countermanded the concept of protein translocation through the β-barrel pore of a single translocation unit. The formation of such a superordinate ring-like structure would lead to a larger lumen than that formed by a single β-barrel and would explain other findings from the same group. Using different single-chain antibody constructs in combination with the IgA1 protease translocation unit, it was demonstrated that folded passenger proteins containing stable disulfide bonds were able to be transported to the cell surface (136, 137). In contrast, superordinate ring-like structures have not been observed for the translocation unit of any other autotransporter protein, in particular those investigated in the natural host background (81). Moreover, conductance measurements with the translocation units of NalP (87) and BrkA (109) in black lipid membranes indicated a smaller pore size than that expected if oligomeric ring-like structures were formed. We propose a different explanation that accommodates all of these somewhat controversial observations. The clearly detectable oligomeric rings and the definite transport of folded domains could be an extraordinary feature of the *Neisseria* IgA1 protease translocation unit expressed in an *E. coli* host background. That the host background can have severe effects on the structure of an autotransporter protein has been exemplified by the *Helicobacter pylori* AlpA autotransporter. AlpA was shown to be processed as a lipoprotein when expressed in *E. coli* DH5α, but no such processing was observed in wild-type *H. pylori* (85). Not only the passenger and the translocation unit but also the signal peptide and the inducible promoter were heterologous in relationship to the *E. coli* host cell. The PelB signal peptide used with the IgA1 protease translocation unit was not a natural constituent of the passengers under investigation, and the inducible promoter used to express the artificial constructs resulted in much more protein in the cell than observed for the IgA1 protease in a natural environment. In the initial experiments using the IgA1 protease translocation unit and CTB as a passenger, the CTB signal peptide was used for transport across the inner membrane and a constitutive promoter was applied to express the different gene constructs (49, 56, 58). This could explain why oligomeric ring-like structures were not observed in these experiments and why it was necessary to avoid disulfide bonds to keep the passenger in a translocation competent state. Even though it is conceivable that the high-level expression of an autotransporter in the heterologous host could result in the formation of oligomeric aggregates, it is rather unlikely that this would result in an alternative export mechanism. A plausible explanation for the proposed translocation of folded domains (136, 137) could also be that the integrity of the outer membrane was damaged under the experimental conditions used, resulting in the artificial accessibility of the passengers to the cell surface. Finally, the hypothesis of ring formation by usher proteins has since been modified, and it is currently accepted that usher proteins act as dimers based on recent investigations (68).

The host background is not the only influence on surface display of recombinant proteins using translocation units from different autotransporters. The structure and the nature of the (recombinant) passenger domain itself, as well as the signal peptide used for inner membrane translocation and the degree of expression induced by the promoter, can strongly influence the results obtained. It appears worthwhile to reconsider the extrapolation of results obtained with more or less artificial systems to the situation found for a natural autotransporter protein in its natural environment.

AUTODISPLAY

An *E. coli* Autotransporter in an *E. coli* Host Background

After discovery of IgA1 protease from *Neisseria gonorrhoeae* and its secretion mechanism, it was quickly concluded that some surface proteins from other gram-negative bacteria could

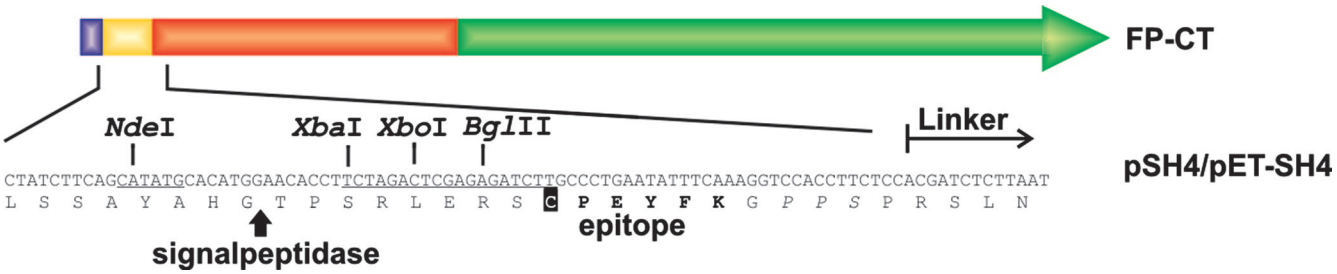

FIG. 3. Structure of an artificial autotransporter protein as used in autodisplay. FP-CT is a cysteine-containing fusion protein that is encoded either by plasmid pSH4 under control of a strong constitutive promoter (P_{TK}) or by plasmid pET-SH4 under the control of the inducible T7/lac promoter. The environments of the passenger insertion site, necessary to obtain surface translocation, are given as sequences. Restriction endonuclease cleavage sites for insertion of passenger-encoding DNA sequences are underlined. Various other restriction sites are available in similar plasmids. The signal peptide originates from CTB, and the signal peptidase cleavage site is marked by an arrow. The signal peptides of PelB, AIDA-I, OmpA, and β-lactamase have also been used in combination with translocation units from different natural autotransporter proteins. The specific cleavage site for IgA1 protease that can be applied for the release of the passenger protein into the extracellular milieu is in italics, and the linear epitope for a mouse monoclonal antibody (Dü142) which can be used for labeling is in bold. The cysteine used in "cystope tagging," a specific labeling and detection method, is indicated by a black box.

be transported by similar means (57). In 1995, 10 surface or secreted proteins from gram-negative bacteria were selected on the basis of common structural features and were combined in a new protein family called autotransporters (48). In that publication, which was the first to mention the term autotransporter, the AIDA-I protein from *E. coli* was identified to be transported in a manner similar to that for the IgA1 protease from *N. gonorrhoeae*. AIDA-I, the adhesin involved in diffuse adherence of enteropathogenic *E. coli* (EPEC) was discovered in 1989 (8) and was the subject of numerous investigations of its structural and functional properties (6–11, 62, 81, 124). In contrast to the IgA1 protease, AIDA-I occurs naturally in *E. coli* and therefore was considered a superior tool for surface display in this homologous host.

We have developed a system for the autotransport of recombinant passengers to the cell surface, which we call the autodisplay system. Autodisplay initially described only the system based on AIDA-I, but there is currently no reason why display systems based on other autotransporters should not also be called autodisplay. We propose that autodisplay should be defined as the recombinant surface display of proteins or peptides by means of an autotransporter in any gram-negative bacterium.

The β-barrel and linker region of AIDA-I was used in the development of the autodisplay system and combined in frame with the signal peptide of CTB and a strong constitutive promoter (P_{TK}) within a medium-copy-number plasmid backbone (73). The signal peptide, promoter, and plasmid vector backbone were identical to those used in the initial experiments investigating surface display by the IgA1 protease autotransporter (55, 56, 58). This provided a better basis to compare the efficiencies of the two surface display systems. P_{TK} is an artificial promoter that was constructed for IgA1 protease-mediated surface display (56). A schematic description of the structure of a typical artificial autotransporter protein used for autodisplay is shown in Fig. 3. The dimensions of the β-barrel of the AIDA-I polyprotein precursor were initially assessed by computer-aided structure prediction (73) and then experimentally verified by investigating the subcellular locations of the identical passenger fused to various portions of the C-terminal part of AIDA-I (74). The minimal linker portion required to reach the cell surface was determined to be 52 amino acids (aa) (73). This minimal linker was used for the surface display of short peptides or proteins with no known fixed three-dimensional structure and for peptide libraries (45). A more extended linker was used for proteins, such as enzymes, where limiting the flexibility could constrain folding and consequently activity (47, 50, 107) (Fig. 4). The linker was extended to the length corresponding to the linker of the natural AIDA-I passenger, which is 160 aa long (124). Protease cleavage sites have been inserted into the linker regions used for autodisplay, to enable the sequence-specific release of the passenger protein into the supernatant. Epitopes have also been inserted to allow detection of the tag via monoclonal antibodies. An antibody-independent detection method, requiring only the addition of a single amino acid, was developed for autodisplay and named "cystope tagging" (46, 51). This is superior to the epitope-tagging strategy, in which 5 to 10 amino acids must be inserted. Cystope tagging is based on the fact that in gram-negative bacteria natural surface proteins, including autotransporters, contain no accessible cysteine residues. The insertion of a single cysteine residue into the linker region (Fig. 3) provides a site for modification, for instance, by maleimide and its derivatives. This specific labeling can be used to detect and verify surface exposure by Western blotting, photometric, or FACS applications (46). Specific labeling of a single cysteine residue within the linker region was shown to work even if the passenger protein contained several cysteine residues (51). This may be because cysteine residues are generally buried and not externally accessible in native proteins such as enzymes. Cystope tagging was successfully applied to follow surface translocation of bovine adrenodoxin (Adx) (five inherent cysteines) (46), sorbitol dehydrogenase (SDH) (three inherent cysteines) from *Rhodobacter sphaeroides* (50, 51), and esterase (two inherent cysteines) from *Salmonella enterica* serovar Typhimurium (51).

As mentioned above, the terminal step in autodisplay requires the translocation of the passenger through a size-limited pore formed by the β-barrel. This maintains a transformation-competent state of the passenger by restricting it from acquiring a stable, three-dimensional conformation during transport (49, 56). Transport is blocked in the periplasm if stable folding

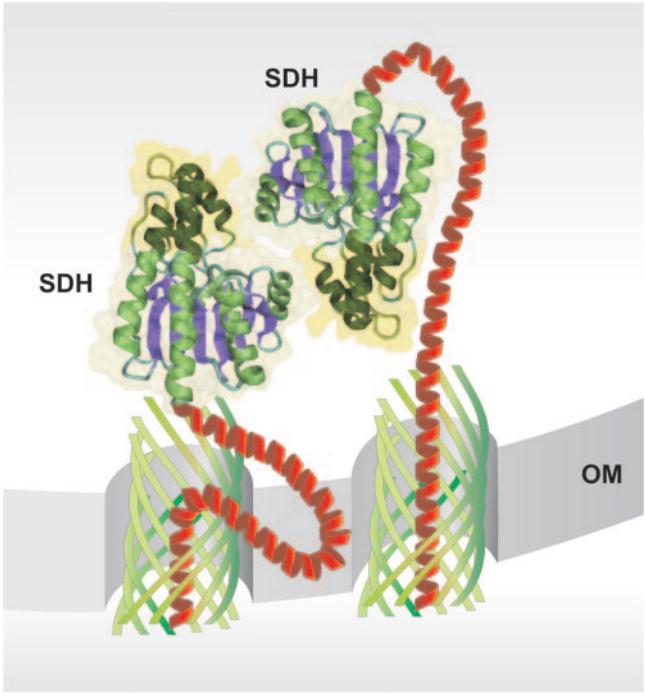

FIG. 4. Passenger-driven dimerization of SDH expressed by autodisplay at the cell surface. Due to the free motility of the β-barrel, serving as an anchor within the outer membrane in autodisplay, passenger proteins can spontaneously form dimers at the cell surface, even when they are expressed as monomers form monomeric genes. This is aided by the high number of recombinant proteins (e.g., SDH) expressed at the cell surface by autodisplay, bringing the monomers in close enough vicinity to interact. It is a unique feature of the autodisplay system and has not been reported for any other surface display system so far.

occurs (52). A wide variety of passenger proteins of biotechnological importance contain disulfide bridges, and these bonds are normally formed in the periplasm of *E. coli*. To facilitate the autodisplay of such proteins, a DsbA-negative mutant strain of *E. coli* (JK321) was constructed (49). The *ompT*-gene in the DsbA-negative strain was mutated in order to obtain stable surface display of the recombinant passenger proteins. Outer membrane protease T (OmpT) is an endopeptidase of *E. coli* and has homologs in a limited set of gram-negative bacteria (32). Naturally, it contributes to bacterial resistance against cationic antimicrobial peptides (33), but it can also be used for the sequence-specific release of recombinant surface proteins into the supernatant. OmpT-negative and OmpT-positive mutant strains of *E. coli* provide an interesting option for autodisplaying recombinant proteins. The surface exposure of the recombinant passenger protein can be verified and quantified in an *ompT*-negative host. Subsequently, the plasmid with the identical autotransporter-passenger gene construct can be expressed in an OmpT-positive host, resulting in the secretion of the passenger into the supernatant (47, 73). The disulfide bonds in a passenger protein need to be formed by spontaneous oxidation at the cell surface in a DsbA-negative host strain (44, 47, 51). It has to be expected, however, that disulfide bond formation by spontaneous oxidation will not be as efficient or accurate as the enzyme-catalyzed reaction in the periplasm, and it cannot be excluded that this may lead to obstacles in the surface display of other disulfide bond-containing proteins.

To summarize, the autodisplay system consists of vectors encoding various artificial autotransporter genes using different parts of the linker region and the β-barrel from AIDA-I. The autodisplay system is highly flexible for application-based adaptation. This flexibility is provided by different modifications of the linker, use of various signal peptides under the control of inducible or constitutive promoters, and mutant strains of *E. coli* supporting transport and surface display by the autotransporter pathway. Methods for detection and tracing of surface translocation are also available, which are independent of the protein domain used as the passenger.

Biotechnical and Biomedical Applications of the Autodisplay System

The various passenger proteins reported to date as having been expressed on the cell surface via autodisplay are listed in Table 1. The initial experiments showing proof of principle for using AIDA-I-based artificial autotransporter constructs to display recombinant passengers on the *E. coli* surface utilized CTB (73, 74) and a linear epitope (PEYFK) (73) for the monoclonal antibody raised against the Nef protein of human immunodeficiency virus (Dü142). CTB was chosen as the passenger for comparative analysis of the efficiency of the autodisplay system since it has been used as a passenger in surface expression studies with various other transporting proteins, including the IgA1 protease (49, 56, 58, 67). Surface expression of both recombinant proteins was of the same order of magnitude as expression of the natural outer membrane proteins, OmpA and OmpF/C. The surface expression of CTB using the homologous AIDA-I protein was estimated to be twice the expression using the IgA1 protease (73). No degradation of the heterologous proteins was detected, and expression of CTB in an OmpT-positive background resulted in its release into the extracellular milieu. Moreover, cells autodisplaying either the epitope or CTB could be used with whole-cell detection methods, including ELISA and immunofluorescence microscopy, indicating that cells remained intact. This result particularly encouraged attempts to autodisplay structurally and functionally more complex proteins on the cell surface.

Autodisplay of enzymes and whole-cell biocatalysis. The spectrum of enzymes displayed at the cell surface by autodisplay spans hydrolases, oxidoreductases, and electron transfer proteins (Table 1).

(i) Hydrolases. The β-lactamase hydrolase was the first example of the surface display of an active enzyme by autodisplay in *E. coli* (65). The β-lactamase protein occurs naturally in the periplasm, confining the challenge of its autodisplay to the last step in transport, the outer membrane translocation (18, 63). Testing the surface display of a naturally occurring periplasmic protein had the additional advantage that its native signal peptide could be used. Considerable amounts of β-lactamase were detectable at the cell surface in the OmpT/DsbA-negative host background. The enzymatic activity was determined to be 0.1 to 0.2 U per 2.5×10^9 bacterial cells using penicillin G as a substrate and was estimated to be approximately 20% of the activity of purified, free β-lactamase. The cell integrity re-

TABLE 1. Autotransporter-mediated surface display of recombinant proteins and peptides in gram-negative bacteria

Autotransporter	Recombinant passenger(s)	Passenger function	Host	Application	Whole-cell analytics	Reference(s)
IgA1 protease	CTB	ND[a]	*S. enterica*[b]	Translocation studies	Immunofluorescence, ELISA	54
			E. coli OmpT$^-$		Immunofluorescence, ELISA	55, 56
			E. coli OmpT$^-$ DsbA$^-$		ND	47
	scFv (anti-His)	+	*E. coli* OmpT$^-$, *E. coli* OmpT$^-$ DsbA$^-$	Translocation studies	Immunofluorescence, ELISA	125, 127
	EETI-II (*E. elaterium* trypsin inhibitor II)	+	*E. coli* DsbA$^-$	Studies on passenger structure	FACS	131
	Mouse MT	+	*E. coli* DsbA$^-$, *R. eutropha*[c]	Heavy metal binding	ELISA	118
			P. putida	Heavy metal binding	ND	119
	Fos/Jun leucine zipper domains	+	*E. coli* OmpT$^-$	Bacterial cell-to-cell adhesion	Immunofluorescence	123
	scFv (anti-TGFV[g])	+	*E. coli* HB2151	TGFV neutralization	ND	124
	Camel V_{HH} domains (antiamylase), scFv (anti-Levan)	+	*E. coli* OmpT$^-$, *E. coli* OmpT$^-$ DsbA$^-$	Translocation studies	ELISA	126
SSP	Pseudoazurin (*A. eutrophus*)	ND	*E. coli* OmpT$^-$	Translocation studies	Immunofluorescence	105
VirG	MalE, PhoA	ND	*E. coli* OmpT$^-$, *E. coli* OmpT$^-$ DsbA$^-$	Translocation studies	ELISA	116
AIDA-I Autodisplay	CTB	ND	*E. coli* OmpT$^-$	Translocation studies	Immunofluorescence, ELISA	70
			E. coli OmpT$^-$ DsbA$^-$			70, 71
Autodisplay	Nef epitope of human immunodeficiency virus (PEYFK)	+	*E. coli* OmpT$^-$	Translocation studies	Immunofluorescence, ELISA	70
			E. coli OmpT$^-$ DsbA$^-$			44
Autodisplay	β-Lactamase	+	*E. coli* OmpT$^-$ DsbA$^-$	Translocation studies	ND	63
Native	LTB (*E. coli*)	ND	*E. coli* OmpT$^-$	Translocation studies	Immunofluorescence	59
Native	T-cell epitopes of HSP60 (*Y. enterocolitica*)	+	*E. coli* OmpT$^-$	Translocation studies, murine T-cell stimulation	Immunofluorescence, ELISA	59
Autodisplay	Bovine adrenodoxin (Adx)	+	*E. coli* OmpT$^-$	Steroid synthesis, whole-cell biocatalysis	FACS	45
						40, 44
Autodisplay	Esterase A (*B. gladioli*)	+	*E. coli* OmpT$^-$	Whole-cell ester hydrolysis	UV/visible spectroscopy	100
Native	InvX (*M. tuberculosis*)	+	*E. coli* OmpT$^-$	HeLa cell attachment, HeLa cell invasion	Immunofluorescence	151
Autodisplay	$HSP60_{74–86}$ epitope (*Y. enterocolitica*)	+	*S. enterica*,[b] *E. coli* OmpT$^-$	Vaccination	Immunofluorescence	62
Autodisplay	UreA and fragments (*H. pylori*)	+	*S. enterica*[b]	Vaccination	ND	91
Autodisplay	SDH *(R. sphaeroides)*	+	*E. coli* OmpT$^-$	Whole-cell biocatalysis	Immunofluorescence, FACS, UV/visible spectroscopy	48, 49
Autodisplay	Aprotinin (bovine pancreatic trypsin inhibitor)	+	*E. coli* OmpT$^-$	Enzyme binding studies	FACS	50
			E. coli OmpT$^-$ DsbA$^-$	Translocation studies	Immunofluorescence	

Continued on following page

TABLE 1—*Continued*

Autotransporter	Recombinant passenger(s)	Passenger function	Host	Application	Whole-cell analytics	Reference(s)
Autodisplay	P15 (human C-reactive protein)	+	*E. coli* OmpT$^-$	Random library screening	FACS, immunofluorescence	42, 43
Native	MalE	ND	*E. coli* ED9	Translocation studies	Immunofluorescence	95
Antigen 43	Chlam12 and CTP3 epitopes	+	*E. coli* HEHA16	Translocation studies	Immunofluorescence	52
	FimH lectin domain	+	*S. enterica*[b]			
MisL	NANP epitope (*Plasmodium falciparum*)	+	*S. enterica*[d], *E. coli* OmpT$^-$	Translocation studies, vaccination	Immunofluorescence, FACS	4, 93
	Shiga toxin B subunit		rEPEC O103:H2	Translocation studies, vaccination	Immunofluorescence	139
VacA	CTB	ND	*H. pylori*	Translocation studies	ND	21
PalA	MBP	ND	*E. coli* BL21(DE3)	Translocation studies	ND	64
EstA I[e]	β-Lactamase	+	*E. coli* OmpT$^-$, *E. coli* OmpT$^-$ DsbA$^-$	Translocation studies	Immunofluorescence, FACS	135
EstA II[f]	Different lipases	+	*E. coli* OmpT$^-$	Translocation studies	FACS	3
EspP	CTB	ND	*E. coli* OmpT$^-$, *E. coli* OmpT$^-$ DsbA$^-$	Translocation studies	ND	106

[a] ND, not determined.
[b] Serovar Typhimurium.
[c] Formerly *Alcaligenes eutrophus*.
[d] Serovars Typhimurium and Typhi.
[e] From *Pseudomonas putida*.
[f] From *Pseudomonas aeruginosa.*
[g] TGFV, transmissible gastroenteritis coronavirus.

mained undisturbed, indicating a clear advantage of autodisplay for the surface expression of β-lactamase over other display systems in *E. coli* (25). These experiments were performed with cells harvested from agar plates as in earlier experiments using the IgA1 protease. We should point out here that the use of solid growth media is not a hindrance in basic research but would be impractical for biotechnical applications.

(ii) Esterases. Among the hydrolases, esterases represent a group of enzymes of great interest for biotechnological and industrial applications (14, 88). They exhibit a broad natural variety of substrates and reaction types. Due to their diverse substrate specificities and their stereoselectivity, esterases have been successfully used in the synthesis of optically pure substances. More recently, esterases have also been used in laboratory approaches to obtain tailor-made biocatalysts (94, 95, 105). It is of striking advantage in the evolutive approach to express the enzyme to be evolved on the surface of a living cell. The first esterase that was autodisplayed in an active form on the surface of *E. coli* was EstA from *Burgholderia gladioli* (107). EstA consists of 351 aa and has a molecular mass of 35.4 kDa. Its coding sequence was inserted between the signal peptide of CTB and the full-length AIDA-I linker region. After detection of the esterase domain on the cell surface, the specific esterase activity of whole cells on the substrate, *p*-nitrophenylacetate, was determined to be 1.7 mU/mg protein. The enzyme activity of whole cells displaying EstA was determined photometrically using an agar plate pH assay in combination with a filter overlay assay employing α-naphthyl acetate as a substrate. This methodology provides an option for the high-throughput screening of enzyme libraries. The viability of *E. coli* cells displaying EstA was not reduced, as measured by the number of CFU. This is a clear advantage of the heterologous surface display of esterases by autodisplay over other systems, in which only 15 to 60% of the CFU were reported, depending on the heterologous esterase displayed (4). Autodisplay could be employed for the surface display of other heterologous esterases (51); however, more recently autotransporter proteins have been discovered which possess an esterase moiety as the natural passenger (66, 144, 146). These proteins may provide, at least in some instances, a simpler method to exploit the synthetic potential of an esterase enzyme displayed at the cell surface.

(iii) SDH. Polyols and sugars are awkward to produce by standard organic synthesis because of the enhanced number of identical functional groups at different positions in these molecules. Biocatalysis using enzymes with high regio- and stereoselectivity could afford a solution (30). For this purpose, SDH from *Rhodobacter sphaeroides* was expressed on the cell surface using autodisplay (50). SDH belongs to the short-chain dehydrogenase/reductase family of proteins and is a dimer with a

subunit molecular mass of 29 kDa (257 aa) (90, 120). Although sorbitol is the preferred substrate, SDH can also utilize other substrates, including the conversion of galactitol into D-tagatose and of L-arabinol into L-ribulose (103). By inserting its coding sequence between those of the CTB signal peptide and a modified linker region, SDH was successfully expressed at the cell surface using autodisplay. In fact, SDH expression exceeded that of the resident outer membrane proteins, OmpF/C and OmpA. Antiserum specific for SDH recognized a protein band twice the size of monomeric SDH in sodium dodecyl sulfate-polyacrylamide gel electrophoresis under nonreducing conditions (without 2-mercaptoethanol). This was a clear indication for the passenger-driven dimerization of monomeric SDH subunits at the cell surface (Fig. 4). This passenger-driven dimerization is a unique feature of autodisplay and has not been observed for any other surface display system to date. SDH has been reported to be a functional dimer as a purified enzyme (90, 120). Based on the absence of interactions fixing the β-barrel to lipids within the membrane, the β-barrel may be assumed to be mobile within the membrane bilayer. Since the AIDA-I β-barrel, which serves as the membrane anchor of the passenger in autodisplay, is mobile within the outer membrane, passenger-driven dimerization or even multimerization should be possible on the *E. coli* surface. The whole-cell biocatalyst obtained by autodisplay of SDH was used for the efficient synthesis of sorbitol (0.11 U/2.5 $\times$ 10^9 cells), fructose (0.11 U), D-tagatose (0.07 U), and L-ribulose (0.15 U) (50). The number of SDH molecules per cell was determined to be 150,000 by specific fluorescein labeling of the SDH molecules on the cell surface and comparing FACS analysis to a calibration curve using beads coated with known numbers of fluorescein molecules. The specific activity of SDH molecules displayed at the cell surface was compared to that of free SDH molecules purified after intracellular expression (120). The specific activity of surface-displayed molecules was only 5% of the activity of free molecules. A similar, although smaller, reduction in activity was observed for β-lactamase. Aside from the reduced molecular flexibility resulting from C-terminal fixation of the enzymes to the linker region, another situation may further reduce enzyme activity in the case of SDH. Many of the lipopolysaccharide (LPS) molecules comprising the outer part of the asymmetric outer membrane are similar to the natural substrates and products of SDH reactions. Competitive enzyme inhibition of SDH oxidoreductase by these molecules could contribute to the reduced enzyme activity. It was also determined that the substrate preference of the surface-displayed SDH was altered in comparison to that of free, purified SDH. Purified SDH preferred sorbitol as a substrate in the oxidation reaction, followed by galactitol and finally arabitol, whereas the whole-cell biocatalyst preferred arabitol, followed by sorbitol and galactitol (50). Both limited flexibility due to linker attachment and competition by LPS molecules probably act in concert to influence the functionality of surface-displayed SDH. We should also point out that folding of the enzyme molecule on the cell surface happens in the absence of chaperones and folding catalysts. Within the cell, protein folding is assisted by chaperones, which prevent misfolding and aggregation. It cannot be excluded that a considerable part of the molecules displayed at the cell surface will misfold in the absence of such chaperones. The absence of folding catalysts, such as DsbA and peptidyl-prolyl *cis*/*trans* isomerases, could also hamper efficient folding of displayed proteins and contribute to reduced enzyme activity.

(iv) Bovine adrenodoxin. The ferredoxin from bovine adrenal cortex, termed adrenodoxin (Adx) (14.4 kDa), belongs to the [2Fe-2S] ferredoxins, a family of small acidic iron-sulfur proteins that are found in bacteria, plants, and animals (31). It plays an essential role in electron transport from adrenodoxin reductase (AdR) to mitochondrial cytochrome P450 enzymes, which are involved in the synthesis of steroid hormones. The iron-sulfur cluster of Adx is coordinated by four sulfur atoms from the side chains of four of its five cysteine residues (80). During heterologous nonsurface expression in *E. coli*, it was shown to be assembled in the cytoplasm as well as in the periplasm (36). Autodisplay of Adx was successfully achieved using the CTB signal peptide and the AIDA-I linker and β-barrel (47). Expression was of the same order of magnitude as that observed for the natural outer membrane protein, OmpA, in the same cell. As observed for SDH, dimeric Adx molecules formed spontaneously with high efficiency on the bacterial cell surface (44). Adx was previously reported to function as a homodimer in electron transfer (91). The dimeric Adx molecules at the cell surface, however, were inactive, and electron spin resonance measurements revealed that they were devoid of the iron-sulfur cluster (47). Since the autotransporter secretion mechanism requires that a protein be transported to the surface in an unfolded state, Adx was transported as apo-Adx without the prosthetic group. The apo-Adx molecules displayed at the cell surface were subsequently activated by the chemical incorporation of the [2Fe-2S] cluster. Iron-sulfur cluster incorporation appeared to work best under anaerobic conditions, when Li_2S was added dropwise to Adx-displaying cells in a ferrous ammonium sulfate buffer at room temperature. Using this procedure, iron-sulfur clusters were formed and incorporated into the apo-Adx displayed at the bacterial surface. Cells survived the procedure well and could be handled afterwards under aerobic conditions without a reduction in activity (47). Subsequent addition of purified AdR and P450 CYP11A1 or P450 CYP11B1 yielded a whole-cell biocatalyst for the efficient synthesis of pregnenolone from cholesterol or of corticosterone from 11-deoxycorticosterone (Fig. 5) (44). Addition of artificial membrane constituents or detergents, which was indispensable in the past for functional steroidal P450 enzymes, was unnecessary. The whole-cell biocatalyst activity (0.21 nmol/h/nmol CYP11A1) was, however, in the same range as that obtained using artificial membrane or detergent systems. Together the results show that whole cells expressing functional Adx molecules on the surface provide a sufficient and more natural environment for P450 enzyme functionality. The whole-cell system developed by autodisplay of Adx is an easy-to-handle and stable tool for the expression of membrane-associated P450 enzymes without the need of microsome preparation or reconstitution of artificial membrane vesicles. Harnessing the biotechnological potential of P450 enzymes is substantially improved by this methodology. As one example, *E. coli* cells expressing Adx at the surface could be supplied with P450 and AdR and then could serve as a whole-cell carrier to target soil requiring detoxification. Cells prepared likewise could also be used in a fermentor to synthesize steroids or produce pharmaceutically important secondary

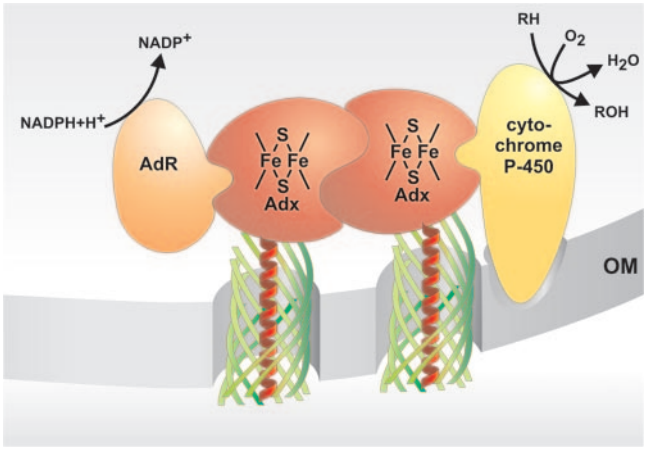

FIG. 5. Whole-cell biocatalyst for the synthesis of steroids obtained by autodisplay of Adx. After transport of apo-Adx to the cell surface, dimers were formed spontaneously and the electron transfer activity of Adx was restored by chemical incorporation of the [2Fe-2S] cluster. After the addition of purified AdR and CYP11A1 or CYP11B1, an efficient whole-cell biocatalyst for the synthesis of pregnenolone or corticosterone, respectively, was obtained. The cell envelope of *E. coli* provided a membrane environment sufficient for both P450 enzymes to be active. OM, outer membrane.

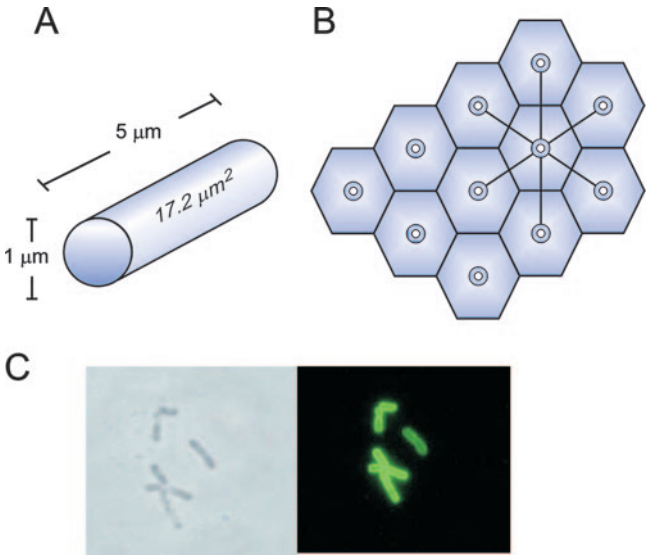

FIG. 6. Distribution of the β-barrels within the outer membrane of *E. coli* by the use of the autodisplay system. (A) The rod-shaped cell of *E. coli* can be idealized as a cylinder with a height of 5 μm and a radius of 0.5 μm. with these values, the entire surface area of a single cell can be calculated to be 17.2 μm^2. (B) The number of active Adx molecules displayed at the surface of a single cell using autodisplay has experimentally been determined to be 180,000. The radius of a single β-barrel can be calculated to be 1.1 nm, which is in congruence with the value derived from the crystal structure of NalP (1.0 nm in one dimension and 1.25 nm in the other). Given that the barrels are evenly spread over the entire surface, the mean distance between two adjacent molecules can be calculated to be 8.4 nm in any dimension by assuming that the expansion space of one barrel has the shape of an equilateral hexagon. (C) *E. coli* cells displaying 180,000 Adx molecules were subjected to indirect immunofluorescence microscopy. After labeling with an anti-Adx rabbit serum and a second anti-rabbit antibody coupled to FITC, cells were analyzed, and no indication was found for a polar distribution of recombinant Adx molecules on the cell surface of *E. coli* as has been reported for the natural passenger of AIDA-I. Rather, the picture obtained accords with an even distribution all over the entire surface.

metabolites from plants or microorganisms. Laboratory evolution could also be simplified, as cells can easily be harvested by centrifugation and, if necessary, distributed in separate reaction chambers. The question arises whether P450s expressed on the *E. coli* surface by the autotransporter pathway could also be active, especially if they are coexpressed with Adx.

Liquid culture conditions were optimized for the surface display of Adx using the autodisplay system, as groundwork for the development of biotechnological applications and large-scale production processes (44). A calibration curve describing the dependency of substrate conversion on the number of Adx molecules was recorded using the substrate conversion rate of CYP11A1 with purified holo-Adx molecules (47). This assay was performed with different numbers of *E. coli* cells displaying Adx instead of holo-Adx, and the number of active Adx molecules displayed at the cell surface was estimated to be 180,000 per cell (47). This number is similar to the number of native OmpA molecules expressed in the outer membrane (reported to be 200,000 copies per cell) and to the number of SDH molecules that were displayed per cell. However, most if not all of the Adx molecules displayed appeared also to be active in electron transport.

The question arises whether the *E. coli* cell envelope is actually capable of incorporating such a tremendous number of recombinant proteins. If we assume for the following theoretical considerations that a single *E. coli* cell is a 1-μm-wide and 5-μm-long cylinder (Fig. 6A), the complete surface area of the cell can be calculated to be approximately 17.2 μm^2. The actual length of an *E. coli* cell, of course, depends on the growth phase and nutrition state and could be in the range of 2 μm for exponentially growing cells. The actual value of the surface area could also be somewhat higher than that of a cylinder, since the *E. coli* surface is assumed to be crumpled, thus increasing its area. The pore size of the NalP β-barrel was determined to be 10 × 12.5 Å from its crystal structure (133).

The overall β-barrel of the AIDA-I autotransporter was calculated according to the method of Murzin et al. (82, 83) to have a radius of approximately 1.1 nm (J. Jose and S. von Schwichow, unpublished). Assuming an equal distribution of the 180,000 Adx molecules detected on the cell surface over the entire cell surface area, the mean distance between two barrels is estimated to be about 8.4 nm in any direction (Fig. 6B). The *E. coli* cell envelope should have no problem incorporating this number of recombinant proteins and, in principle, should be capable of absorbing more than four times this number. The mean distance of 8.4 nm between barrels within the outer membrane has another interesting implication. The lateral diffusion coefficient for membrane proteins in fibroblasts at room temperature was determined to be 2.6×10^{-10} $cm^2\ s^{-1}$ (23). There is no experimental evidence that lateral diffusion rates in the fibroblast plasma membrane and the bacterial outer membrane are comparable. However, using this value for the lateral diffusion of a β-barrel within the outer membrane of *E. coli*, it would take less than 34 μs to bring two barrels into contact by accident. It appears reasonable that Adx dimers form spontaneously from the monomers fused to the

AIDA-I β-barrel on the cell surface, using this estimation for diffusion (44). This estimation can be taken as only a rough approximation, since the lateral diffusion coefficient for membrane proteins, which usually contain α-helices, in the fibroblast plasma membrane is not exactly transferable to the β-barrel proteins within the outer bacterial membrane. The lateral diffusion coefficient of LPS in *Salmonella enterica* serovar Typhimurium was experimentally determined to range between 2.0×10^{-10} cm^2 s^{-1} (104) and 2.9×10^{-13} cm^2 s^{-1} (79). Recent investigations point out that the determination of these values was strongly influenced by experimental conditions, such as the LPS chain length or the fluorescent dye used to monitor movement (29). Nevertheless, using lateral diffusion coefficients in this range for a β-barrel protein within the outer membrane, two passenger proteins anchored within the outer membrane by a β-barrel would still only need much less than 1 second to meet. Interestingly, the investigation of LPS diffusion (29) showed that, at least in growing cells, proteins are not evenly distributed on the *E. coli* cell wall but are organized into helical ribbons that span the length of this gram-negative rod. The LPS O antigen especially appeared to be virtual immobile within these helical ribbons, indicating the existence of stable lateral interactions between tightly woven LPS molecules. Four forces can be taken into account for this high degree of organization: interconnection of LPS molecules by divalent cations, hydrogen bonding, interactions between the O polysaccharides of neighboring molecules, and van der Waals attractions between fatty acid chains. Although free diffusion of LPS was hampered by these interactions, no mechanical obstacles appeared to hamper protein diffusion into broad areas of the walls or the poles of the cell. It was suggested that diffusible proteins were not part of stable helices formed by LPS. Although the view of an *E. coli* outer membrane comprised of a homogeneous surface with evenly distributed LPS molecules, phospholipids, and an abundance of proteins has changed to a membrane displaying areas of distinct composition, the accidental concourse of two single proteins within this surface still appears to be an event of high probability which should occur within a very short time frame.

More recently it has been shown that the natural, unmodified autotransporter proteins IcsA and SepA of *Shigella flexneri*, BrkA of *Bordetella pertussis*, and AIDA-I of *E. coli* are localized at the bacterial pole (42). All of these autotransporters also exhibited a polar localization in the cytoplasm prior to secretion, and interestingly, NalP of the diplococcal *Neisseria meningitidis* also showed a polar localization in *E. coli*, whereas in the authentic host, it was secreted at distinct spots of the cell. The restriction of autotransporter proteins to the cell pole was shown to be dependent on the presence of complete LPS. When the K-12 *E. coli* strain, which lacks complete LPS, was used instead of wild-type *E. coli* as the host for recombinant expression, an even distribution of the AIDA-I autotransporter over the bacterial surface was observed. Obviously LPS plays an important role in the localization of autotransporter proteins on the cell surface, perhaps due to formation of distinct barriers in the outer membrane in line with the observations discussed above. The polar localization of a passenger protein was never observed in the autodisplay system (Fig. 6C). This is in good agreement with the results discussed above, since most experiments utilized K-12 derivatives rather than wild-type *E. coli* as hosts for recombinant protein expression. Protein distribution appears to be a host strain-specific phenomenon, which reinforces the importance of carefully choosing the host strain according to the nature of the investigation. The autotransporter protein distribution on the cell surface could also be influenced by the artificial combination of domains from different origins in the recombinant protein. The autodisplay system combines the CTB signal peptide with the recombinant passenger and the translocation unit and linker region of AIDA-I. At least three of the natural autotransporters showing a polar localization, BrkA, AIDA-I, and IcsA, possess an unusually long signal sequence (89, 126). Extended signal sequences of this type have been reported to be associated exclusively with autotransporter proteins larger than 100 kDa (38). Not only were these extended signal peptides shown to target SecA via the SecB molecular chaperone, but evidence was also found for targeting the passenger to the signal recognition particle (SRP) pathway independent of SecB, thus permitting a cotranslational membrane translocation of the precursor (89, 126). Finally, it has recently been shown that the Sec translocon is organized in an inner membrane helix along the length of *E. coli* (113).

Autodisplay allows a tremendous number of active molecules ($>10^5$ per cell) to be displayed on the cell surface without hampering cell viability. This result is unprecedented and unique among all other bacterial and surface display systems applied so far. Furthermore, autodisplay provides novel and efficient access to the very interesting synthetic potential of the membrane-associated P450 enzymes. Adx autodisplay was also the first report of the cellular surface display of a recombinant, heterologous protein with an inorganic prosthetic group.

Autodisplay of enzyme inhibitors and library screening. A unique feature of the autodisplay system is its application as a tool in drug discovery (45). This challenging application is basically comprised of three steps: (i) surface display of peptide libraries, (ii) labeling of single cells with an inhibitor structure by target enzyme binding, and (iii) selecting and sorting of labeled cells by FACS (Fig. 7). The rationale of this concept is based on the idea that a typical enzyme inhibitor has a high affinity for its target enzyme and vice versa. The inhibitor-target enzyme affinity can be exploited to specifically label *E. coli* cells displaying an active inhibitor at the cell surface. If the enzyme is coupled to a fluorescent dye, flow cytometry can be used to sort single cells expressing an inhibitor with affinity for the enzyme. The selected cells can subsequently be used for clonal production of cell quantities sufficient for analytical or preparative purposes. This concept takes advantage of the high copy number of each molecule expressed on the *E. coli* cell surface using the autodisplay system and of the good viability and integrity of these cells. The first advantage enhances the selection of positive from negative variants, and the latter is crucial for the number of clones surviving the FACS sorting (45).

The first step towards using autodisplay in drug discovery was to show that an enzyme inhibitor can be expressed in an active conformation at the *E. coli* surface. Aprotinin (62 aa), a rapidly folding serine protease inhibitor stabilized by three disulfide bonds (2, 19), was chosen as a passenger for autodisplay (52). A detectable amount of aprotinin was expressed at the cell surface under reducing conditions to diminish the

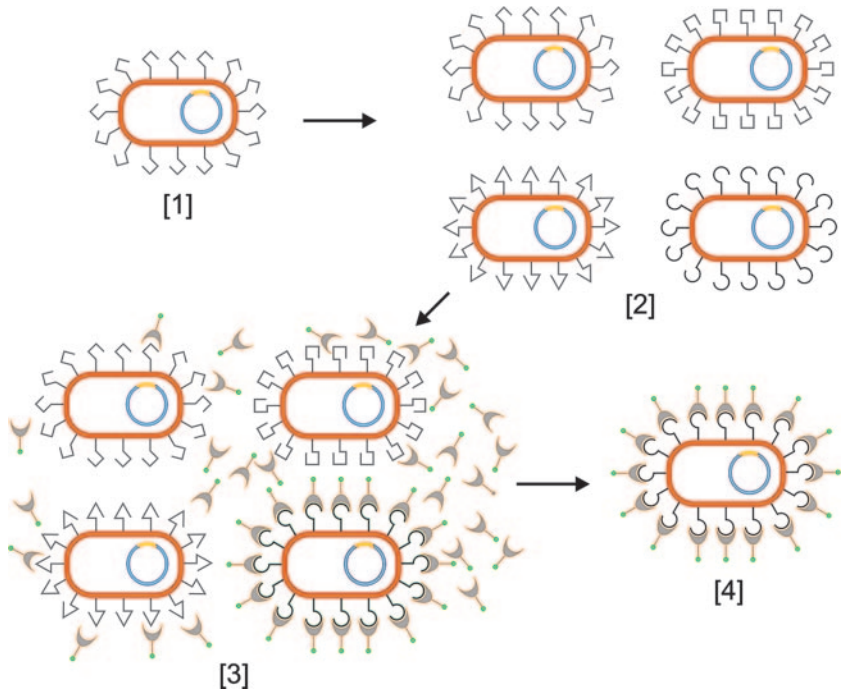

FIG. 7. Surface display library screening to identify new enzyme inhibitors by autodisplay. (1) A peptide that is known to be an inhibitor (the lead) is expressed at the cell surface by autodisplay and tested for functionality. (2) Random libraries are generated by standard genetic engineering tools, where each cell of *E. coli* displays one distinct variant in high numbers. (3) The library of *E. coli* cells with different variants is screened by target enzyme labeling. Since an enzyme inhibitor has high affinity to its target enzyme and as a consequence the enzyme has high affinity to the inhibitor as well, the target enzyme will bind to an inhibiting structure expressed at the cell surface. If the target enzyme is coupled to a fluorescent dye (e.g., FITC), the cell displaying the appropriate variant can be sorted by FACS. (4) The cell selected by this procedure can be used for clonal production of cell quantities sufficient for, e.g., DNA sequence analysis and hence for the identification of a new lead structure.

degree of disulfide bond formation in the periplasm. Aprotinin has been previously shown to be a strong inhibitor (K_i of 3.5 μM) of human leukocyte elastase (75). Bacterial cells displaying aprotinin were able to specifically bind human leukocyte elastase, and this binding could be quantified by flow cytometric analysis. These results showed for the first time that it is indeed possible to label cells of *E. coli* expressing an inhibitor at the cell surface by its affinity to the target enzyme (52). Autodisplay of aprotinin, however, appeared not to be quantitative. Considerable amounts of the protease inhibitor were lost during transport to the cell surface, which was most probably due to a very rapid adoption of a transport-incompatible three-dimensional structure in the periplasm and subsequent degradation by the periplasmic protease machinery. Assay conditions were optimized to reduce this effect. However, aprotinin was not a good candidate for constructing random libraries to identify new inhibitors, as the effects of random mutations on enzyme inhibition were not clearly distinguishable from effects of premature folding and consequent reduction of aprotinin at the cell surface.

A protease inhibitor with a less stable three-dimensional structure, P15, was investigated as a model inhibitor in autodisplay (45). P15 consists of 15 aa and is derived from the human C-reactive protein, whose serum concentration increases during acute inflammation. It has been shown to be a strong inhibitor of human cathepsin G, with a K_i of 0.25 μM (147, 148). Cathepsin G is assumed to be an important target in the treatment of chronic inflammatory diseases, such as rheumatoid arthritis or pulmonary emphysema (98). Cathepsin G was also reported more recently to activate matrix metalloproteinase 2 (108), which plays an important role in tumor invasion. P15 could be expressed in larger amounts than aprotinin on the *E. coli* cell surface by autodisplay (45). The expression level was in the same range as that of the resident OmpA outer membrane protein, and cells displaying P15 could be efficiently labeled with human cathepsin G coupled to fluorescein isothiocyanate (FITC). This second example of a successful target enzyme labeling of cells displaying an inhibitor could be easily quantified using FACS (45). Moreover, cells displaying P15 could be sorted from a mixed population with an excess of control cells displaying a noninhibiting peptide. The selected cells survived sorting without loss and were grown to single-cell clones to be used for DNA sequence analysis and studies on protein expression. Autodisplay of an enzyme inhibitor with subsequent target enzyme labeling and FACS is a reliable method to sort cells displaying an active inhibitory structure at the surface. This method was subsequently used to screen a random surface display library consisting of 1.15×10^5 different variants, and three new peptide inhibitors of cathepsin G were identified. The most active inhibitor was P6, with a 50% inhibitory concentration of 11.7 μM (45). Using P15 and cathepsin G as a model inhibitor and target enzyme, respectively, a new labeling procedure by fluorescence coupling of the target enzyme was developed, which is the essential element for drug discovery using autodisplay. Using repeated cycles of surface display of random libraries and FACS of positive

clones, a gradual optimization that is congruent with the idea of directed evolution is possible. Autodisplay may be a promising tool for performing laboratory evolution to improve the inhibitory potential of peptides. This strategy can probably be applied for inhibitors of enzymes other than proteases or for the investigation of any receptor-ligand relationship, but further experiments to test these potential application areas will be needed.

Autodisplay of epitopes and vaccine development. In addition to the surface display of enzymes and enzyme inhibitors, the cellular surface display of epitopes and antigens is a promising application of autodisplay. The Nef epitope of the human immunodeficiency virus was one of the two initial passenger proteins expressed in the autodisplay system (73). In earlier studies concerning whole-cell vaccine development, it was shown that the secretion of antigens resulted in an improved immune protection compared to that with intracellularly expressed antigens (34, 39, 43). It can be extrapolated that the autodisplay of epitopes could result in enhanced stimulation of the immune system and that epitope autodisplay could be used to generate live oral vaccine vectors as vaccine carriers. T-cell epitopes of *Yersinia enterocolitica* heat shock protein 60 (HSP60) have been expressed on the surface of attenuated *Salmonella* vaccine strains (64) and *E. coli* strains using autodisplay and the unmodified AIDA-I autotransporter (61). T cells isolated from mice immunized with *Salmonella* cells displaying HSP60 exhibited an antigen-specific proliferation which was accompanied by high-level gamma interferon secretion. This indicates an effective immune stimulation by the vaccine strains orally distributed to C57BL/6 mice and demonstrates the applicability of autodisplay of antigenic determinants for live attenuated *Salmonella* vaccine strain development. *E. coli* cells displaying epitopes of HSP60 could be used to directly stimulate antigen-specific T-cell clones from mice immunized with HSP60 in an in vitro assay. AIDA-I-mediated surface display could also be applied for the B subunit of the heat-labile enterotoxin of *E. coli* (LTB), another antigenic determinant (61). More recently, autodisplay was used to express antigenic urease fragments from *Helicobacter pylori* on the surface of *Salmonella enterica* serovar Typhimurium vaccine strains for the subsequent oral immunization of specific-pathogen-free female BALB/c mice (96). This resulted in a significant reduction in the *H. pylori* burden after challenge infection and an increased protective efficacy in the murine *Helicobacter* infection model. Taken together, these results indicate that autodisplay increases the immunogenicity of recombinant antigens expressed on oral live vaccine strains, and they show the feasibility of immunizing against *H. pylori* with *Salmonella* vaccine strains displaying T-cell epitopes by autodisplay.

SURFACE DISPLAY OF RECOMBINANT PROTEINS BY OTHER AUTOTRANSPORTERS

The translocation units of the IgA1 protease from *N. gonorrhoeae* and of AIDA-I from *E. coli* are the most extensively used examples for the surface display of recombinant proteins by autotransporter proteins. The number of different proteins from various origins and with various functions translocated by the AIDA-I protein, in its entirety or in part, is impressive. AIDA-I appears promising for future applications based on these results. Beside these two examples, several autotransporters have been exploited for the surface display of recombinant proteins, including SSP from *Serratia marcescens* (112), IcsA (formerly VirG) from *Shigella flexneri* (125), the antigen 43 protein of *E. coli* (54), MisL from *Salmonella enterica* serovar Typhimurium (99, 100, 150), EstA from *P. putida* (146), PalA from a not-further-classified *Pseudomonas* species (66), EstA from *P. aeruginosa* (4), VacA from *H. pylori* (22), and EspP from *E. coli* (114) (Table 1). The *Serratia marcescens* protease (SSP) was discovered almost concurrently with the IgA1 protease as an outer membrane protein (145), and its C-terminal part was shown to play a role in the surface translocation of the protease precursor (78, 110, 111). However, it was used as a carrier for the surface display of a recombinant protein for the first and the last time in 1994 (112). Pseudoazurin (123 aa) from *Alcaligenes faecalis* was chosen as a passenger protein. It belongs to the family of cupredoxins, naturally contains copper, and serves as a direct electron donor for the reduction of NO_2^- by the nitrite reductase from *A. faecalis*. The efficient surface display of this recombinant protein in *E. coli* using the SSP translocation unit, as well as its extracellular release in an OmpT-positive host cell background, was clearly shown, but no data about the copper content and electron transfer activity of the protein at the cell surface were reported. That study can be regarded as a proof of principle for the SSP-mediated surface display of recombinant proteins in *E. coli*, but more investigation is required for it to be useful for biotechnological or biomedical exploitation. On the whole, investigations of the surface display of recombinant proteins by autotransporter proteins other than the IgA1 protease and AIDA-I had the primary aim to study how the passenger was translocated to the cell surface and did not concentrate on investigating the use of whole cells displaying recombinant protein for application purposes. In the style of the early experiments with the IgA1 protease, CTB was used as a passenger for surface display mediated by VacA from *H. pylori* (22) and EspP from *E. coli* (114), and the influence of folding during transport was investigated. IcsA was used for the surface display of the natural periplasmic proteins maltose binding protein (MBP) (MalE) and alkaline phosphate (PhoA) (125). Transport and surface processing were clearly shown for both passengers, but no data were reported about activity. An MBP was also used in studies investigating PalA-mediated surface display, but no data about the protein functionality were reported (66). An enzymatically active β-lactamase was displayed at the cell surface using the *P. putida* EstA as a carrier in *E. coli* (146). Using the translocation domains of antigen 43, it was possible also to display the lectin moiety of FimH with detectable D-mannose binding activity in *E. coli* (54).

More prominent examples of the biomedical and biotechnological application of cells with autotransporter-mediated surface display of recombinant proteins have been reported for MisL from *Salmonella* and EstA from *P. aeruginosa*. MisL was used for the surface display of the 4-aa immunodominant B-cell epitope (Asn-Ala-Asn-Pro [NANP]) of the circumsporozoite protein from *Plasmodium falciparum*. Surface display of the epitope was demonstrated in *Salmonella* serovar Typhimurium as well as in *S. enterica* serovar Typhi, and a significant

immune response was obtained from immunization of mice with either live vector (100). In a follow-up investigation, two passengers consisting of either 8 or 53 repeats of the NANP tetrapeptide were constructed, and efficient surface display and the release of the passenger proteins were shown in *Salmonella* and *E. coli* (99). Another group demonstrated the surface display of a variant containing eight NANP repeats by MisL in the isogenic *ler* (LEE-encoded regulator) mutant of *E. coli* (recombinant EPEC [rEPEC] O103:H), which was shown to be attenuated and immunogenic in mice. Using an identical strategy for the surface display of the Shiga toxin B subunit (Stx1B), however, did not result in significant protection of rabbits after inoculation with rEPEC mutant cells bearing this construct (150).

The use of lipases for the hydrolysis of racemic esters is a well established method for obtaining enantiomeric pure compounds. Lipases have the ability not only to hydrolyze but also to synthesize many different esters with high specificity and regio- and enantioselectivity under mild conditions. For these reasons, they represent biocatalysts of strong interest for pharmaceutical, organic chemistry, and biotechnological applications. The EstA lipase from *P. aeruginosa* was used as a system for the surface display of different lipases, including LipA from *Bacillus subtilis*, cutinase from *Fusarium solani pisi*, and *S. marcescens* lipase (4). In contrast to other attempts for the surface display of enzymes, the EstA domain was not replaced by the various lipase domains within the polyprotein precursor in this system. Here, the recombinant lipases were inserted in front of the EstA domain, and the serine residue in the active site of EstA was changed into alanine using site-directed mutagenesis in order to distinguish between the lipolytic activities of EstA and the passenger lipase domains. This strategy would have resulted in relatively large proteins to be transported and displayed at the cell surface. All fusion constructs with the recombinant lipase domains were detectable at the cell surface and exhibited significant enzymatic activities. However, the viability of the cells displaying the different lipases was strongly reduced, as only 60% of the *S. marcescens* lipase cells, 30% of cutinase cells, and 15% of LipA cells survived in comparison to control cells. The reduced cell viability in these experiments may have resulted from the uncommonly large size of the displayed proteins, as well as the use of the PhoA signal peptide and the heterologous host background (a *Pseudomonas* gene was expressed in an *E. coli* host background). Nevertheless, if cell viability could be improved in this system, it could provide an interesting platform for the directed evolution of this important biocatalyst class of lipases, especially if used in combination with high-throughput readout systems for selecting improved variants (3).

PERSPECTIVES ON THE APPLICATION OF THE AUTODISPLAY SYSTEM

The autodisplay system has some striking advantages in comparison to the other surface display systems described to date. The first advantage is the large number of recombinant proteins displayed on the surface of *E. coli*. Based on the electron transfer activity of bovine Adx (47) or a procedure for specific labeling of SDH from *R. sphaeroides* (50) displayed at the cell surface, the number of recombinant molecules was determined to be in the range of 1.5×10^4 to 1.8×10^5 per cell. This was significantly more than has been reported for the Lpp-OmpA hybrid system in *E. coli* (range of 1×10^5 to 5×10^4 per cell) (24) and the fibronectin binding protein-based system in *Staphylococcus carnosus* (10^3 to 10^4 per cell) (123). Exact numbers for other surface display systems have not yet been reported. In the autodisplay system, most of the passenger proteins can be easily detected by sodium dodecyl sulfate-polyacrylamide gel electrophoresis followed by Coomassie brilliant blue staining. Moreover, the staining intensity can be compared to that of the resident outer membrane protein A. It has been reported that 2×10^5 molecules of OmpA are expressed at the surface of each cell (60). In most cases, the expression level of the recombinant protein as indicated by its staining intensity was identical to or even exceeded that of OmpA. All in all, this indicates that autodisplay enables the recombinant expression of more than 10^5 protein or peptide molecules on the surface of a single *E. coli* cell. One exception was observed in the autodisplay of aprotinin (52). Other proteins containing cysteine or disulfide bonds, such as CTB, Adx, SDH, or different esterases were efficiently transported in the DsbA-negative mutant *E. coli*, JK321, with or without the optimization of the medium components. Under all tested conditions, only small amounts of aprotinin could be expressed at the cell surface. A plausible explanation is that most of the aprotinin molecules could not be prevented from folding during transport. The acquisition of a rigid tertiary conformation in the periplasm would have resulted in blockage of transport across the pore formed by the β-barrel and subsequent degradation by the periplasmic proteases DegP and DegQ. This emphasizes a crucial point in autodisplay of recombinant proteins. Namely, passenger proteins must remain in an unfolded conformation to maintain a transport-competent state (49, 56) and in order to be displayed at the cell surface in adequate numbers with high reproducibility (52, 125).

A second striking advantage of the autodisplay system is the mobility of the β-barrel serving as an anchor for the recombinant protein within the outer membrane. This enables passenger proteins, which are expressed as monomers within the context of the autodisplay system, to form functional dimers at the cell surface, as observed for the autodisplay of Adx and SDH (47, 50). Such a passenger-driven, spontaneous dimerization of surface-exposed domains has not yet been reported for any other surface display system investigated. Theoretically, the stable dimers of Adx and SDH on the cell surface after autodisplay could have been formed via a dimerization of the β-barrel as well. However, dimer formation was never observed for proteins known to be monomers inherently after expression at the cell surface by autodisplay, and more recent cross-linking experiments with the AIDA-I β-barrel indicated that it is present primarily as a monomer and not as a dimer or oligomer (81). Taking these results together, it appears rather unlikely that dimerization at the cell surface is driven by the β-barrel. Passenger-driven dimerization offers interesting prospects for future applications of the autodisplay system. Other interesting proteins known to be functional as dimers, such as eukaryotic receptors or transcription factors, could be displayed in an active form at the cell surface of *E. coli*. The system could also be used for the surface expression of heterodimeric proteins by expressing each monomer as a single

fusion with the domains needed for autodisplay in the same cell. The two artificial genes needed in this case could be carried either by one plasmid or by two plasmids belonging to different incompatibility groups. Formation of the heterodimers at the cell surface should appear spontaneously, as observed for the homodimers of Adx or SDH. Finally, the present point of view does not exclude the possibility that higher degrees of association, such as trimers, tetramers, or even hexamers, could be obtained at the cell surface using the autodisplay system. This possibility is under current investigation.

Another outstanding characteristic of the autodisplay system is the possibility of incorporating an inorganic prosthetic group into an apoprotein expressed at the cell surface of *E. coli*, as was successfully reported for the [2Fe-2S] cluster of bovine Adx (44, 47). Cells displaying the apoprotein were subjected to a one-step, single-vial procedure under anaerobic conditions and could be subsequently used under aerobic conditions without loss of cell viability or electron transfer activity. The functional surface display of proteins requiring inorganic cofactors has not been reported for any other surface display system to date. Autodisplay may have promise as a method of functional surface display of other proteins containing cofactors, such as P450 enzymes, flavin adenine dinucleotide, flavin mononucleotide, or metal ion-containing proteins. More experimentation with each specific target will be required before these goals can be realized. In particular, heme-containing P450 enzymes would be of great commercial importance, as they are involved in the synthesis of a wide variety of valuable compounds and the degradation of numerous toxic compounds (12). It is worth emphasizing that in the whole-cell biocatalyst for the P450-mediated steroid synthesis obtained using autodisplay of Adx, the cell envelope of *E. coli* provided a membrane environment sufficient for functional P450 enzymes (44). The P450 enzymes are innate membrane-associated proteins (12). Autodisplay of P450 enzymes could open a new dimension in the development of whole-cell factories, with the aim of using enzyme-coated cells for applications, including P450-mediated drug metabolism studies.

Finally, the most convenient feature of autodisplay is that surface expression of large numbers of recombinant proteins does not reduce cell viability or integrity (45, 47, 50, 73). Cells survived challenging analytic approaches, including FACS. This distinction enables selection of single cells having a specific feature from a library of variants and clonal expansion for sequence determination or structural analysis of the molecule displayed at the cell surface. This strategy was successfully applied for the identification of new cathepsin G inhibitors from random peptide libraries and is a first indication that the high number of molecules displayed on the surface of a single cell combined with persistent cell integrity could afford direct selection of cells displaying the correct molecules from a library (45) instead of requiring enrichment or panning positive cells (13, 142). Currently, random libraries of esterases have been successfully created and expressed at the cell surface using autodisplay (J. Jose et al., submitted for publication). The surface display library construction using autodisplay could even be extended to combinatorial approaches which take advantage of the ability of dimer formation of peptides or proteins displayed at the cell surface.

The autodisplay system has proven to be an efficient tool for the surface display of a wide variety of recombinant proteins in *E. coli* and perhaps generally in gram-negative bacteria. To date, its applications span the functional surface display of enzymes, enzyme inhibitors, and antigens or receptors; the development of whole-cell biocatalysts or biofactories; and peptide library screening by target enzyme binding. Future experiments will focus on its further application for analytical or preparative purposes. The heterologous nature of the artificial gene construct may influence the efficiency of protein expression at the cell surface using the autodisplay system (Fig. 3). However, these obstacles exist for any other surface display system investigated so far as well, and therefore autodisplay can be considered an attractive tool for the surface expression of recombinant proteins.

COMPENDIUM

Autotransporter proteins are versatile tools for the surface display of recombinant proteins. This is documented by the large number of different recombinant proteins and autotransporters used for this purpose (Table 1). Whole cells displaying the recombinant passengers could be subjected to various analytical processes and used for biotechnical applications, such as whole-cell biocatalysis or bioremediation, and for biomedical applications, including vaccination or virus inactivation. The surface display of a recombinant protein by an autotransporter can be achieved by simply replacing the coding sequence of the natural passenger with the gene of the protein to be displayed. In most, if not all, examples discussed in this review, the foreign gene insertion was accompanied by some deliberate or inadvertent alterations that deserve closer investigation. The natural autotransporter proteins are usually expressed in their natural host background at very low levels, which are too low for most targeted applications with recombinant passengers. Therefore, the investigations of the surface display of recombinant proteins using an autotransporter were performed with the introduction of either strong constitutive promoters (44, 45, 47, 49, 52, 55, 56, 58, 73, 74, 107) or inducible promoters (46, 50, 51, 101, 130, 131, 134–138, 142). The strong expression of the recombinant passenger-autotransporter protein fusion could interfere with cell viability and with the integrity of the outer membrane. Additionally, the unnaturally high density of protein molecules could result in interactions on the cell surface or en route to the cell surface, which are not possible under native autotransporter function. This is of no concern as long as the biotechnological or biomedical application works, but it must be taken into consideration if the application does not work as conceptualized or if these results are being used to draw conclusions about the native autotransporter secretion mechanism in general.

The second important issue in the surface display of recombinant proteins by the autotransporter pathway is the use of the signal peptide. The signal peptide guides the first step in transport, the crossing of the inner cytoplasmic membrane. The natural signal peptide of the autotransporter protein was used in only a few of the cases described here (16, 61, 114). The most frequently used signal sequences or leader peptides were those of CTB (22, 44, 46, 47, 49–53, 55, 56, 58, 64, 65, 73, 74,

96, 107) and PelB (pectate lyase B) (61, 130, 131, 134–138). The leader peptide of CTB had proven value in the initial experiments investigating IgA1 protease-mediated surface display of recombinant passengers (56, 58), which led to its use in similar experiments with other autotransporter proteins. Its successful use for the functional surface display of eukaryotic passengers and passenger proteins normally localized in the cytoplasm confirmed its suitability. The PelB leader peptide is included in commercially available vectors and has been extensively used in the phage display of recombinant proteins (121). PelB is a natural protein of the periplasm and, as such, presents a good alternative for cell surface translocation studies using autotransporters, because transport across the inner membrane would be facilitated by its own leader peptide and should not be a problem. The periplasmic proteins MalE (66, 101, 125), PhoA (125), β-lactamase (146), and pseudoazurin (112) have been investigated in the context of their own signal sequences but with different autotransporters. Signal sequences that were used with other passenger proteins include those of PhoA (4), of the *E. coli* LTB (100), and of OmpA (74). The signal sequences of OmpA, MalE, PhoA, and PelB have been reported to target the Sec pathway. Nothing is known about the CTB signal peptide in this respect. From its primary sequence, it appears to more closely resemble the signal peptides that are known to target the SRP pathway, such as Sfm or TolB. Interestingly, this is also true for the LTB signal sequence used with the MisL autotransporter. Recent studies of the unusually long signal sequences of different natural autotransporters have revealed that they could target either the Sec or the SRP pathway, depending on the conditions and their sequence content (89, 126), and that some of the proteins bearing such signal sequences exhibit preferred expression at the cell poles (42). It must be assumed that the signal sequences contain more information than simply what is needed for traversing the inner membrane. Again, this is of no importance as long as the desired biotechnical or biomedical task is fulfilled, but it can be relevant if the knowledge gained using the artificial constructs in the surface display of recombinant proteins is extrapolated to the natural situation.

Two other domains contribute to the effectiveness of the surface display of recombinant proteins by the autotransporter pathway, the linker and the β-barrel. All computer-aided approaches predicted that both termini of the β-barrel are located on the same side of the membrane, namely, on the inner surface directed towards the periplasm. Indirect experimental evidence was gathered subsequently for this (74), and final proof came from the first crystal structure of an autotransporter protein (133). Because of this conformation, a stretch of amino acids that penetrates the barrel channel and affords full surface exposure of the passenger domain is required. This sequence was determined to comprise 52 aa in the AIDA-I autotransporter using protease accessibility studies (73). The crystal structure of NalP showed this structure to consist of 32 aa and to exhibit an α-helical structure (133). This helix, which is located in the primary sequence N terminal to the barrel domain, positions the C terminus of the passenger domain at the extracellular surface of the outer membrane. Different names are used for this sequence in the literature, including the α-domain, β_2-domain, linking region, or simply helix. As it links the passenger domain with the β-barrel, the name "linker" was chosen in the initial experiments with the IgA1 protease and has been used for this reason in this review. Whereas the designation of the linker region in the surface display of recombinant proteins is quite simple because it is the region linking the recombinant passenger with the β-barrel, it is much more difficult to identify in natural autotransporter proteins. For those natural autotransporter proteins which are proteolytically cleaved, whether autoproteolytically or not, and released into the supernatant, it appears to be justified to refer to the remaining portion of the protein anchored within the outer membrane by the β-barrel as the linker region. For natural autotransporter proteins displayed on the cell surface, it is a nontrivial task to distinguish between the so-called passenger domain and the linker region. Evidently, the α-helix located in the lumen of the β-barrel is an inherent part of the linker region, but in most cases, the linker region appears to reach beyond the α-helical passenger domain. It is questionable, though, whether allocating a "junction region" (86) will help to better define the boundary of the linker region.

The 52-aa region that has been shown experimentally, for the AIDA-I autotransporter, to be the minimal length of the linker to run through the hydrophilic pore formed by the β-barrel (73, 74) is sufficient for the surface display of recombinant peptides (45) and permits the folding of complex structures (52). Recent investigations revealed the presence of an intramolecular chaperone domain within the region between the β-barrel and passenger in BrkA (86), AIDA-I (62, 101), and other autotransporter proteins (38). No homologous domain has yet been identified in any other protein different from autotransporters, with the exception of some bacterial toxins. It appears not to be necessary for the surface display of functional recombinant proteins by the AIDA-I translocation unit. It can, however, in at least some recombinant passenger proteins, considerably improve the yield of surface display (74), which may be critical for certain biotechnological applications. It could be important for folding after transport or maintenance in an unfolded state during transport to the cell surface and could have coevolved with its natural passenger domains. BrkA and AIDA-I belong to the group of unusually large autotransporter proteins, which could require the involvement of an autochaperone. Therefore, a more systematic approach could unearth the truth about this particular domain in the function of the autotransporter-mediated surface display. For instance, one could conceive of using an identical (large) passenger domain with an identical signal peptide and β-barrel within the context of the same promoter and vector copy number but altering the size and primary structural features of the linker. Similar experiments could be conducted to more closely assess the other domains involved, including the signal peptide and β-barrel, as well as the passenger gene sequences utilized. Such investigations may help to unify the controversial results obtained in different investigations of the transport or nontransport of folded domains. A third concept involves an outer membrane helper protein, Omp85, in outer membrane translocation during the autotransporter secretion (87, 139, 140). This hypothesizes that the β-barrel containing the α-helical linker in its channel could be the structure at the end of the process and not necessarily imply that the passenger was transported across the channel as well, leaving the door open for folded protein translocation (87).

Finally, relatively few data are available concerning the structure-transport activity relationship of the β-barrel in the surface display of recombinant proteins. Only a few site-directed mutagenesis or deletion experiments have been performed (66, 74). As a crude rule, it is preferable to use the translocation unit within a homologous host species background, such as an *E. coli* autotransporter within an *E. coli* host. The use of an autotransporter in a species that is phylogenetically not closely related to its natural host, such as using a *Pseudomonas* autotransporter in an *E. coli* host (4) or a *Neisseria* autotransporter in *E. coli* (138), can interfere with cell viability or outer membrane integrity, whereas the use of the closely related *Salmonella* as a host organism with an *E. coli* autotransporter is obviously unproblematic (54, 64, 96). *E. coli* is not, a priori, an optimal host organism for any application. *Pseudomonas* or *Ralstonia* species could be much more robust host organisms for the surface display of enzymes or binding proteins for antipollution applications (130, 131). In these cases, it appears worthwhile to investigate whether a homologous autotransporter protein (i.e., a *Pseudomonas* autotransporter in a *Pseudomonas* host background) could be beneficial. Even though some details remain controversial and require further thorough investigation, the concepts concerning the surface display of recombinant proteins by the autotransporter pathway are clear, and the successful examples of their biotechnological and biomedical applications promise exciting developments in the near future.

REFERENCES

1. **Adams, T. M., A. Wentzel, and H. Kolmar.** 2005. Intimin-mediated export of passenger proteins requires maintenance of a translocation-competent conformation. J. Bacteriol. **187:**522–533.
2. **Barbar, E., G. Barany, and C. Woodward.** 1996. Unfolded BPTI variants with a single disulfide bond have diminished non-native structure distant from the crosslink. Fold. Des. **1:**65–76.
3. **Becker, S., H. U. Schmoldt, T. M. Adams, S. Wilhelm, and H. Kolmar.** 2004. Ultra-high-throughput screening based on cell-surface display and fluorescence-activated cell sorting for the identification of novel biocatalysts. Curr. Opin. Biotechnol. **15:**323–329.
4. **Becker, S., S. Theile, N. Heppeler, A. Michalczyk, A. Wentzel, S. Wilhelm, K. E. Jaeger, and H. Kolmar.** 2005. A generic system for the *Escherichia coli* cell-surface display of lipolytic enzymes. FEBS Lett. **579:**1177–1182.
5. **Benhar, I.** 2001. Biotechnological applications of phage and cell display. Biotechnol. Adv. **19:**1–33.
6. **Benz, I., S. Knochenhauer, and M. A. Schmidt.** 1990. Molecular mechanisms of adherence of enteropathogenic *Escherichia coli*. Z. Gastroenterol. Verh. **25:**67–70.
7. **Benz, I., and M. A. Schmidt.** 1992. AIDA-I, the adhesin involved in diffuse adherence of the diarrhoeagenic *Escherichia coli* strain 2787 (O126:H27), is synthesized via a precursor molecule. Mol. Microbiol. **6:**1539–1546.
8. **Benz, I., and M. A. Schmidt.** 1989. Cloning and expression of an adhesin (AIDA-I) involved in diffuse adherence of enteropathogenic *Escherichia coli*. Infect. Immun. **57:**1506–1511.
9. **Benz, I., and M. A. Schmidt.** 1990. Diffuse adherence of enteropathogenic *Escherichia coli* strains. Res. Microbiol. **141:**785–786.
10. **Benz, I., and M. A. Schmidt.** 1993. Diffuse adherence of enteropathogenic *Escherichia coli* strains—processing of AIDA-I. Zentbl. Bakteriol. **278:**197–208.
11. **Benz, I., and M. A. Schmidt.** 1992. Isolation and serologic characterization of AIDA-I, the adhesin mediating the diffuse adherence phenotype of the diarrhea-associated *Escherichia coli* strain 2787 (O126:H27). Infect. Immun. **60:**13–18.
12. **Bernhardt, R.** 1996. Cytochrome P450: structure, function, and generation of reactive oxygen species. Rev. Physiol. Biochem. Pharmacol. **127:**137–221.
13. **Bessette, P. H., J. J. Rice, and P. S. Daugherty.** 2004. Rapid isolation of high-affinity protein binding peptides using bacterial display. Protein Eng. Des. Sel. **17:**731–739.
14. **Bornscheuer, U. T.** 2002. Microbial carboxyl esterases: classification, properties and application in biocatalysis. FEMS Microbiol. Rev. **26:**73–81.
15. **Breinig, F., and M. J. Schmitt.** 2002. Spacer-elongated cell wall fusion proteins improve cell surface expression in the yeast *Saccharomyces cerevisiae*. Appl. Microbiol. Biotechnol. **58:**637–644.
16. **Casali, N., M. Konieczny, M. A. Schmidt, and L. W. Riley.** 2002. Invasion activity of a *Mycobacterium tuberculosis* peptide presented by the *Escherichia coli* AIDA autotransporter. Infect. Immun. **70:**6846–6852.
17. **Charbit, A., J. C. Boulain, A. Ryter, and M. Hofnung.** 1986. Probing the topology of a bacterial membrane protein by genetic insertion of a foreign epitope; expression at the cell surface. EMBO J. **5:**3029–3037.
18. **Chervaux, C., N. Sauvonnet, A. Le Clainche, B. Kenny, A. L. Hung, J. K. Broome-Smith, and I. B. Holland.** 1995. Secretion of active beta-lactamase to the medium mediated by the *Escherichia coli* haemolysin transport pathway. Mol. Gen. Genet. **249:**237–245.
19. **Creighton, T. E.** 1992. The disulfide folding pathway of BPTI. Science **256:**111–114.
20. **Daugherty, P. S., B. L. Iverson, and G. Georgiou.** 2000. Flow cytometric screening of cell-based libraries. J. Immunol. Methods **243:**211–227.
21. **Davey, H. M., and D. B. Kell.** 1996. Flow cytometry and cell sorting of heterogeneous microbial populations: the importance of single-cell analyses. Microbiol. Rev. **60:**641–696.
22. **Fischer, W., R. Buhrdorf, E. Gerland, and R. Haas.** 2001. Outer membrane targeting of passenger proteins by the vacuolating cytotoxin autotransporter of *Helicobacter pylori*. Infect. Immun. **69:**6769–6775.
23. **Fisher, K. A., and W. Stoeckenius.** 1982. Membrane models. Springer, Berlin, Germany.
24. **Francisco, J. A., R. Campbell, B. L. Iverson, and G. Georgiou.** 1993. Production and fluorescence-activated cell sorting of *Escherichia coli* expressing a functional antibody fragment on the external surface. Proc. Natl. Acad. Sci. USA **90:**10444–10448.
25. **Francisco, J. A., C. F. Earhart, and G. Georgiou.** 1992. Transport and anchoring of beta-lactamase to the external surface of *Escherichia coli*. Proc. Natl. Acad. Sci. USA **89:**2713–2717.
26. **Freudl, R., S. MacIntyre, M. Degen, and U. Henning.** 1986. Cell surface exposure of the outer membrane protein OmpA of *Escherichia coli* K-12. J. Mol. Biol. **188:**491–494.
27. **Gentschev, I., H. Mollenkopf, Z. Sokolovic, J. Hess, S. H. Kaufmann, and W. Goebel.** 1996. Development of antigen-delivery systems, based on the *Escherichia coli* hemolysin secretion pathway. Gene **179:**133–140.
28. **Georgiou, G., C. Stathopoulos, P. S. Daugherty, A. R. Nayak, B. L. Iverson, and R. Curtiss III.** 1997. Display of heterologous proteins on the surface of microorganisms: from the screening of combinatorial libraries to live recombinant vaccines. Nat. Biotechnol. **15:**29–34.
29. **Ghosh, A. S., and K. D. Young.** 2005. Helical disposition of proteins and lipopolysaccharide in the outer membrane of *Escherichia coli*. J. Bacteriol. **187:**1913–1922.
30. **Giffhorn, F., S. Kopper, A. Huwig, and S. Freimund.** 2000. Rare sugars and sugar-based synthons by chemo-enzymatic synthesis. Enzyme Microb. Technol. **27:**734–742.
31. **Grinberg, A. V., F. Hannemann, B. Schiffler, J. Muller, U. Heinemann, and R. Bernhardt.** 2000. Adrenodoxin: structure, stability, and electron transfer properties. Proteins **40:**590–612.
32. **Grodberg, J., and J. J. Dunn.** 1988. *ompT* encodes the *Escherichia coli* outer membrane protease that cleaves T7 RNA polymerase during purification. J. Bacteriol. **170:**1245–1253.
33. **Guina, T., E. C. Yi, H. Wang, M. Hackett, and S. I. Miller.** 2000. A PhoP-regulated outer membrane protease of *Salmonella enterica* serovar Typhimurium promotes resistance to alpha-helical antimicrobial peptides. J. Bacteriol. **182:**4077–4086.
34. **Haddad, D., S. Liljeqvist, S. Kumar, M. Hansson, S. Stahl, H. Perlmann, P. Perlmann, and K. Berzins.** 1995. Surface display compared to periplasmic expression of a malarial antigen in *Salmonella typhimurium* and its implications for immunogenicity. FEMS Immunol. Med. Microbiol. **12:**175–186.
35. **Halter, R., J. Pohlner, and T. F. Meyer.** 1984. IgA protease of *Neisseria gonorrhoeae*: isolation and characterization of the gene and its extracellular product. EMBO J. **3:**1595–1601.
36. **Hannemann, F., A. K. Bera, B. Fischer, M. Lisurek, K. Teuchner, and R. Bernhardt.** 2002. Unfolding and conformational studies on bovine adrenodoxin probed by engineered intrinsic tryptophan fluorescence. Biochemistry **41:**11008–11016.
37. **Henderson, I. R., R. Cappello, and J. P. Nataro.** 2000. Autotransporter proteins, evolution and redefining protein secretion. Trends Microbiol. **8:**529–532.
38. **Henderson, I. R., F. Navarro-Garcia, M. Desvaux, R. C. Fernandez, and D. Ala'Aldeen.** 2004. Type V protein secretion pathway: the autotransporter story. Microbiol. Mol. Biol. Rev. **68:**692–744.
39. **Hess, J., A. Dreher, I. Gentschev, W. Goebel, C. Ladel, D. Miko, and S. H. Kaufmann.** 1996. Protein p60 participates in intestinal host invasion by *Listeria monocytogenes*. Zentbl. Bakteriol. **284:**263–272.
40. **Isticato, R., G. Cangiano, H. T. Tran, A. Ciabattini, D. Medaglini, M. R. Oggioni, M. De Felice, G. Pozzi, and E. Ricca.** 2001. Surface display of recombinant proteins on *Bacillus subtilis* spores. J. Bacteriol. **183:**6294–6301.
41. **Jacob-Dubuisson, F., R. Fernandez, and L. Coutte.** 2004. Protein secretion

through autotransporter and two-partner pathways. Biochim. Biophys. Acta **1694:**235–257.
42. **Jain, S., P. van Ulsen, I. Benz, M. A. Schmidt, R. Fernandez, J. Tommassen, and M. B. Goldberg.** 2006. Polar localization of the autotransporter family of large bacterial virulence proteins. J. Bacteriol. **188:**4841–4850.
43. **Janssen, R., and J. Tommassen.** 1994. PhoE protein as a carrier for foreign epitopes. Int. Rev. Immunol. **11:**113–121.
44. **Jose, J., R. Bernhardt, and F. Hannemann.** 2002. Cellular surface display of dimeric Adx and whole cell P450-mediated steroid synthesis on *E. coli*. J. Biotechnol. **95:**257–268.
45. **Jose, J., D. Betscheider, and D. Zangen.** 2005. Bacterial surface display library screening by target enzyme labeling: identification of new human cathepsin G inhibitors. Anal. Biochem. **346:**258–267.
46. **Jose, J., and S. Handel.** 2003. Monitoring the cellular surface display of recombinant proteins by cysteine labeling and flow cytometry. Chembiochem. **4:**396–405.
47. **Jose, J., F. Hannemann, and R. Bernhardt.** 2001. Functional display of active bovine adrenodoxin on the surface of *E. coli* by chemical incorporation of the 2Fe-2S cluster. Chembiochem. **2:**695–701.
48. **Jose, J., F. Jahnig, and T. F. Meyer.** 1995. Common structural features of IgA1 protease-like outer membrane protein autotransporters letter. Mol. Microbiol. **18:**378–380.
49. **Jose, J., J. Kramer, T. Klauser, J. Pohlner, and T. F. Meyer.** 1996. Absence of periplasmic DsbA oxidoreductase facilitates export of cysteine-containing passenger proteins to the *Escherichia coli* cell surface via the Iga beta autotransporter pathway. Gene **178:**107–110.
50. **Jose, J., and S. von Schwichow.** 2004. Autodisplay of active sorbitol dehydrogenase (SDH) yields a whole cell biocatalyst for the synthesis of rare sugars. Chembiochem. **5:**100–108.
51. **Jose, J., and S. von Schwichow.** 2004. "Cystope tagging" for labeling and detection of recombinant protein expression. Anal. Biochem. **331:**267–274.
52. **Jose, J., and D. Zangen.** 2005. Autodisplay of the protease inhibitor aprotinin in *Escherichia coli*. Biochem. Biophys. Res. Commun. **333:**1218–1226.
53. **Jung, H. C., J. M. Lebeault, and J. G. Pan.** 1998. Surface display of *Zymomonas mobilis* levansucrase by using the ice-nucleation protein of Pseudomonas syringae 5. Nat. Biotechnol. **16:**576–580.
54. **Kjaergaard, K., H. Hasman, M. A. Schembri, and P. Klemm.** 2002. Antigen 43-mediated autotransporter display, a versatile bacterial cell surface presentation system. J. Bacteriol. **184:**4197–4204.
55. **Klauser, T., J. Kramer, K. Otzelberger, J. Pohlner, and T. F. Meyer.** 1993. Characterization of the Neisseria Iga beta-core. The essential unit for outer membrane targeting and extracellular protein secretion. J. Mol. Biol. **234:**579–593.
56. **Klauser, T., J. Pohlner, and T. F. Meyer.** 1990. Extracellular transport of cholera toxin B subunit using Neisseria IgA protease beta-domain: conformation-dependent outer membrane translocation. EMBO J. **9:**1991–1999.
57. **Klauser, T., J. Pohlner, and T. F. Meyer.** 1993. The secretion pathway of IgA protease-type proteins in gram-negative bacteria. Bioessays **15:**799–805.
58. **Klauser, T., J. Pohlner, and T. F. Meyer.** 1992. Selective extracellular release of cholera toxin B subunit by *Escherichia coli*: dissection of Neisseria Iga beta-mediated outer membrane transport. EMBO J. **11:**2327–2335.
59. **Klemm, P., and M. A. Schembri.** 2000. Fimbriae-assisted bacterial surface display of heterologous peptides 3. Int. J. Med. Microbiol. **290:**215–221.
60. **Koebnik, R., K. P. Locher, and P. Van Gelder.** 2000. Structure and function of bacterial outer membrane proteins: barrels in a nutshell 2. Mol. Microbiol. **37:**239–253.
61. **Konieczny, M. P., M. Suhr, A. Noll, I. B. Autenrieth, and M. Alexander Schmidt.** 2000. Cell surface presentation of recombinant (poly-) peptides including functional T-cell epitopes by the AIDA autotransporter system. FEMS Immunol. Med. Microbiol. **27:**321–332.
62. **Konieczny, M. P. J., I. Benz, B. Hollinderbaumer, C. Beinke, M. Niederweis, and M. A. Schmidt.** 2001. Modular organization of the AIDA autotransporter translocator: the N-terminal beta1-domain is surface-exposed and stabilizes the transmembrane beta2-domain. Antonie van Leeuwenhoek **80:**19–34.
63. **Kornacker, M. G., and A. P. Pugsley.** 1990. The normally periplasmic enzyme beta-lactamase is specifically and efficiently translocated through the *Escherichia coli* outer membrane when it is fused to the cell-surface enzyme pullulanase. Mol. Microbiol. **4:**1101–1109.
64. **Kramer, U., K. Rizos, H. Apfel, I. B. Autenrieth, and C. T. Lattemann.** 2003. Autodisplay: development of an efficacious system for surface display of antigenic determinants in *Salmonella* vaccine strains. Infect. Immun. **71:**1944–1952.
65. **Lattemann, C. T., J. Maurer, E. Gerland, and T. F. Meyer.** 2000. Autodisplay: functional display of active beta-lactamase on the surface of *Escherichia coli* by the AIDA-I autotransporter. J. Bacteriol. **182:**3726–3733.
66. **Lee, H. W., and S. M. Byun.** 2003. The pore size of the autotransporter domain is critical for the active translocation of the passenger domain. Biochem. Biophys. Res. Commun. **307:**820–825.
67. **Lee, S. Y., J. H. Choi, and Z. Xu.** 2003. Microbial cell-surface display. Trends Biotechnol. **21:**45–52.
68. **Li, H., L. Qian, Z. Chen, D. Thibault, G. Liu, T. Liu, and D. G. Thanassi.** 2004. The outer membrane usher forms a twin-pore secretion complex. J. Mol. Biol. **344:**1397–1407.
69. **Liljeqvist, S., P. Samuelson, M. Hansson, T. N. Nguyen, H. Binz, and S. Stahl.** 1997. Surface display of the cholera toxin B subunit on *Staphylococcus xylosus* and *Staphylococcus carnosus*. Appl. Environ. Microbiol. **63:**2481–2488.
70. **Loveless, B. J., and M. H. Saier, Jr.** 1997. A novel family of channel-forming, autotransporting, bacterial virulence factors. Mol. Membr. Biol. **14:**113–123.
71. **Lu, Z., B. C. Tripp, and J. M. McCoy.** 1998. Displaying libraries of conformationally constrained peptides on the surface of *Escherichia coli* as flagellin fusions. Methods Mol. Biol. **87:**265–280.
72. **Malmborg, A. C., E. Soderlind, L. Frost, and C. A. Borrebaeck.** 1997. Selective phage infection mediated by epitope expression on F pilus. J. Mol. Biol. **273:**544–551.
73. **Maurer, J., J. Jose, and T. F. Meyer.** 1997. Autodisplay: one-component system for efficient surface display and release of soluble recombinant proteins from *Escherichia coli*. J. Bacteriol. **179:**794–804.
74. **Maurer, J., J. Jose, and T. F. Meyer.** 1999. Characterization of the essential transport function of the AIDA-I autotransporter and evidence supporting structural predictions. J. Bacteriol. **181:**7014–7020.
75. **McBride, J. D., H. N. Freeman, and R. J. Leatherbarrow.** 1999. Selection of human elastase inhibitors from a conformationally constrained combinatorial peptide library. Eur. J. Biochem. **266:**403–404 12.
76. **Meng, G., N. K. Surana, J. W. St. Geme III, and G. Waksman.** 2006. Structure of the outer membrane translocator domain of the *Haemophilus influenzae* Hia trimeric autotransporter. EMBO J. **25:**2297–2304.
77. **Meyer, T. F., R. Halter, and J. Pohlner.** 1987. Mechanism of extracellular secretion of an IgA protease by gram-negative host cells. Adv. Exp. Med. Biol. **216B:**1271–1281.
78. **Miyazaki, H., N. Yanagida, S. Horinouchi, and T. Beppu.** 1989. Characterization of the precursor of *Serratia marcescens* serine protease and COOH-terminal processing of the precursor during its excretion through the outer membrane of *Escherichia coli*. J. Bacteriol. **171:**6566–6572.
79. **Muhlradt, P. F., J. Menzel, J. R. Golecki, and V. Speth.** 1974. Lateral mobility and surface density of lipopolysaccharide in the outer membrane of *Salmonella typhimurium*. Eur. J. Biochem. **43:**533–539.
80. **Muller, A., J. J. Muller, Y. A. Muller, H. Uhlmann, R. Bernhardt, and U. Heinemann.** 1998. New aspects of electron transfer revealed by the crystal structure of a truncated bovine adrenodoxin, Adx(4–108). Structure **6:**269–280.
81. **Muller, D., I. Benz, D. Tapadar, C. Buddenborg, L. Greune, and M. A. Schmidt.** 2005. Arrangement of the translocator of the autotransporter adhesin involved in diffuse adherence on the bacterial surface. Infect. Immun. **73:**3851–3859.
82. **Murzin, A. G., A. M. Lesk, and C. Chothia.** 1994. Principles determining the structure of beta-sheet barrels in proteins. I. A theoretical analysis. J. Mol. Biol. **236:**1369–1381.
83. **Murzin, A. G., A. M. Lesk, and C. Chothia.** 1994. Principles determining the structure of beta-sheet barrels in proteins. II. The observed structures. J. Mol. Biol. **236:**1382–1400.
84. **Nguyen, T. N., M. Hansson, S. Stahl, T. Bachi, A. Robert, W. Domzig, H. Binz, and M. Uhlen.** 1993. Cell-surface display of heterologous epitopes on *Staphylococcus xylosus* as a potential delivery system for oral vaccination. Gene **128:**89–94.
85. **Odenbreit, S., M. Till, D. Hofreuter, G. Faller, and R. Haas.** 1999. Genetic and functional characterization of the alpAB gene locus essential for the adhesion of *Helicobacter pylori* to human gastric tissue. Mol. Microbiol. **31:**1537–1548.
86. **Oliver, D. C., G. Huang, E. Nodel, S. Pleasance, and R. C. Fernandez.** 2003. A conserved region within the *Bordetella pertussis* autotransporter BrkA is necessary for folding of its passenger domain. Mol. Microbiol. **47:**1367–1383.
87. **Oomen, C. J., P. Van Ulsen, P. Van Gelder, M. Feijen, J. Tommassen, and P. Gros.** 2004. Structure of the translocator domain of a bacterial autotransporter. EMBO J. **23:**1257–1266.
88. **Panda, T., and B. S. Gowrishankar.** 2005. Production and applications of esterases. Appl. Microbiol. Biotechnol. **67:**160–169.
89. **Peterson, J. H., R. L. Szabady, and H. D. Bernstein.** 2006. An unusual signal peptide extension inhibits the binding of bacterial presecretory proteins to the signal recognition particle, trigger factor, and the SecYEG complex. J. Biol. Chem. **281:**9038–9048.
90. **Philippsen, A., T. Schirmer, M. A. Stein, F. Giffhorn, and J. Stetefeld.** 2005. Structure of zinc-independent sorbitol dehydrogenase from *Rhodobacter sphaeroides* at 2.4 A resolution. Acta Crystallogr. D **61:**374–379.
91. **Pikuleva, I. A., K. Tesh, M. R. Waterman, and Y. Kim.** 2000. The tertiary structure of full-length bovine adrenodoxin suggests functional dimers. Arch. Biochem. Biophys. **373:**44–55.
92. **Pohlner, J., R. Halter, K. Beyreuther, and T. F. Meyer.** 1987. Gene structure and extracellular secretion of *Neisseria gonorrhoeae* IgA protease. Nature **325:**458–462.

93. **Pohlner, J., T. Klauser, E. Kuttler, and R. Halter.** 1992. Sequence-specific cleavage of protein fusions using a recombinant *Neisseria* type 2 IgA protease. Biotechnology **10:**799–804.
94. **Reetz, M. T.** 2000. Evolution in the test tube as a means to create enantioselective enzymes for use in organic synthesis. Sci. Prog. **83:**157–172.
95. **Reetz, M. T., S. Wilensek, D. Zha, and K. E. Jaeger.** 2001. Directed evolution of an enantioselective enzyme through combinatorial multiple-cassette mutagenesis. Angew. Chem. Int. **40:**3589–3591.
96. **Rizos, K., C. T. Lattemann, D. Bumann, T. F. Meyer, and T. Aebischer.** 2003. Autodisplay: efficacious surface exposure of antigenic UreA fragments from *Helicobacter pylori* in *Salmonella* vaccine strains. Infect. Immun. **71:**6320–6328.
97. **Robert, V., E. B. Volokhina, F. Senf, M. P. Bos, P. Van Gelder, and J. Tommassen.** 2006. Assembly factor Omp85 recognizes its outer membrane protein substrates by a species-specific C-terminal motif. PLoS Biol. **4:**e377.
98. **Rosalki, S. B.** 2001. C-reactive protein. Int. J. Clin. Pract. **55:**269–270.
99. **Ruiz-Olvera, P., F. Ruiz-Perez, N. V. Sepulveda, A. Santiago-Machuca, R. Maldonado-Rodriguez, G. Garcia-Elorriaga, and C. Gonzalez-Bonilla.** 2003. Display and release of the *Plasmodium falciparum* circumsporozoite protein using the autotransporter MisL of *Salmonella enterica*. Plasmid **50:**12–27.
100. **Ruiz-Perez, F., R. Leon-Kempis, A. Santiago-Machuca, G. Ortega-Pierres, E. Barry, M. Levine, and C. Gonzalez-Bonilla.** 2002. Expression of the *Plasmodium falciparum* immunodominant epitope (NANP)(4) on the surface of *Salmonella enterica* using the autotransporter MisL. Infect. Immun. **70:**3611–3620.
101. **Rutherford, N., M. E. Charbonneau, F. Berthiaume, J. M. Betton, and M. Mourez.** 2006. The periplasmic folding of a cysteineless autotransporter passenger domain interferes with its outer membrane translocation. J. Bacteriol. **188:**4111–4116.
102. **Samuelson, P., M. Hansson, N. Ahlborg, C. Andreoni, F. Gotz, T. Bachi, T. N. Nguyen, H. Binz, M. Uhlen, and S. Stahl.** 1995. Cell surface display of recombinant proteins on *Staphylococcus carnosus*. J. Bacteriol. **177:**1470–1476.
103. **Schauder, S., K. H. Schneider, and F. Giffhorn.** 1995. Polyol metabolism of *Rhodobacter sphaeroides*: biochemical characterization of a short-chain sorbitol dehydrogenase. Microbiology **141:**1857–1863.
104. **Schindler, M., M. J. Osborn, and D. E. Koppel.** 1980. Lateral diffusion of lipopolysaccharide in the outer membrane of *Salmonella typhimurium*. Nature **285:**261–263.
105. **Schmidt, M., M. Baumann, E. Henke, M. Konarzycka-Bessler, and U. T. Bornscheuer.** 2004. Directed evolution of lipases and esterases. Methods Enzymol. **388:**199–207.
106. **Schreuder, M. P., A. T. Mooren, H. Y. Toschka, C. T. Verrips, and F. M. Klis.** 1996. Immobilizing proteins on the surface of yeast cells. Trends Biotechnol. **14:**115–120.
107. **Schultheiss, E., C. Paar, H. Schwab, and J. Jose.** 2002. Functional esterase surface display by the autotransporter pathway in *Escherichia coli*. J. Mol. Catal. **18:**89–97.
108. **Shamamian, P., J. D. Schwartz, B. J. Pocock, S. Monea, D. Whiting, S. G. Marcus, and P. Mignatti.** 2001. Activation of progelatinase A (MMP-2) by neutrophil elastase, cathepsin G, and proteinase-3: a role for inflammatory cells in tumor invasion and angiogenesis. J. Cell Physiol. **189:**197–206.
109. **Shannon, J. L., and R. C. Fernandez.** 1999. The C-terminal domain of the *Bordetella pertussis* autotransporter BrkA forms a pore in lipid bilayer membranes. J. Bacteriol. **181:**5838–5842.
110. **Shikata, S., K. Shimada, H. Kataoka, S. Horinouchi, and T. Beppu.** 1992. Detection of large COOH-terminal domains processed from the precursor of *Serratia marcescens* serine protease in the outer membrane of *Escherichia coli*. J. Biochem. **111:**627–632.
111. **Shikata, S., K. Shimada, Y. Ohnishi, S. Horinouchi, and T. Beppu.** 1993. Characterization of secretory intermediates of *Serratia marcescens* serine protease produced during its extracellular secretion from *Escherichia coli* cells. J. Biochem. (Tokyo) **114:**723–731.
112. **Shimada, K., Y. Ohnishi, S. Horinouchi, and T. Beppu.** 1994. Extracellular transport of pseudoazurin of *Alcaligenes faecalis* in *Escherichia coli* using the COOH-terminal domain of *Serratia marcescens* serine protease. J. Biochem. **116:**327–334.
113. **Shiomi, D., M. Yoshimoto, M. Homma, and I. Kawagishi.** 2006. Helical distribution of the bacterial chemoreceptor via colocalization with the Sec protein translocation machinery. Mol. Microbiol. **60:**894–906.
114. **Skillman, K. M., T. J. Barnard, J. H. Peterson, R. Ghirlando, and H. D. Bernstein.** 2005. Efficient secretion of a folded protein domain by a monomeric bacterial autotransporter. Mol. Microbiol. **58:**945–958.
115. **Smith, G. P.** 1985. Filamentous fusion phage: novel expression vectors that display cloned antigens on the virion surface. Science **228:**1315–1317.
116. **Smith, G. P., and V. A. Petrenko.** 1997. Phage display. Chem. Rev. **97:**391–410.
117. **Stahl, S., A. Robert, E. Gunneriusson, H. Wernerus, F. Cano, S. Liljeqvist, M. Hansson, T. N. Nguyen, and P. Samuelson.** 2000. Staphylococcal surface display and its applications. Int. J. Med. Microbiol. **290:**571–577.
118. **Stathopoulos, C., G. Georgiou, and C. F. Earhart.** 1996. Characterization of *Escherichia coli* expressing an Lpp′OmpA(46–159)-PhoA fusion protein localized in the outer membrane. Appl. Microbiol. Biotechnol. **45:**112–119.
119. **Steidler, L., J. Viaene, W. Fiers, and E. Remaut.** 1998. Functional display of a heterologous protein on the surface of *Lactococcus lactis* by means of the cell wall anchor of *Staphylococcus aureus* protein A. Appl. Environ. Microbiol. **64:**342–345.
120. **Stein, M. A., A. Schafer, and F. Giffhorn.** 1997. Cloning, nucleotide sequence, and overexpression of *smoS*, a component of a novel operon encoding an ABC transporter and polyol dehydrogenases of *Rhodobacter sphaeroides* Si4. J. Bacteriol. **179:**6335–6340.
121. **Steiner, D., P. Forrer, M. T. Stumpp, and A. Pluckthun.** 2006. Signal sequences directing cotranslational translocation expand the range of proteins amenable to phage display. Nat. Biotechnol. **24:**823–831.
122. **St. Geme, J. W., III, and D. Cutter.** 2000. The *Haemophilus influenzae* Hia adhesin is an autotransporter protein that remains uncleaved at the C terminus and fully cell associated. J. Bacteriol. **182:**6005–6013.
123. **Strauss, A., and F. Gotz.** 1996. In vivo immobilization of enzymatically active polypeptides on the cell surface of *Staphylococcus carnosus*. Mol. Microbiol. **21:**491–500.
124. **Suhr, M., I. Benz, and M. A. Schmidt.** 1996. Processing of the AIDA-I precursor: removal of AIDAc and evidence for the outer membrane anchoring as a beta-barrel structure. Mol. Microbiol. **22:**31–42.
125. **Suzuki, T., M. C. Lett, and C. Sasakawa.** 1995. Extracellular transport of VirG protein in *Shigella*. J. Biol. Chem. **270:**30874–30880.
126. **Szabady, R. L., J. H. Peterson, K. M. Skillman, and H. D. Bernstein.** 2005. An unusual signal peptide facilitates late steps in the biogenesis of a bacterial autotransporter. Proc. Natl. Acad. Sci. USA **102:**221–226.
127. **Thanassi, D. G., E. T. Saulino, M. J. Lombardo, R. Roth, J. Heuser, and S. J. Hultgren.** 1998. The PapC usher forms an oligomeric channel: implications for pilus biogenesis across the outer membrane. Proc. Natl. Acad. Sci. USA **95:**3146–3151.
128. **Tommassen, J.** 2007. Biochemistry. Getting into and through the outer membrane. Science **317:**903–904.
129. **Ueda, M., and T. A.** 2000. Genetic immobilization of proteins on the yeast cell surface. Biotechnol. Adv. **18:**121–140.
130. **Valls, M., S. Atrian, V. de Lorenzo, and L. A. Fernandez.** 2000. Engineering a mouse metallothionein on the cell surface of Ralstonia eutropha CH34 for immobilization of heavy metals in soil. Nat. Biotechnol. **18:**661–665.
131. **Valls, M., V. de Lorenzo, R. Gonzalez-Duarte, and S. Atrian.** 2000. Engineering outer-membrane proteins in Pseudomonas putida for enhanced heavy-metal bioadsorption. J. Inorg. Biochem. **79:**219–223.
132. **Van der Vaart, J. M., R. te Biesebeke, J. W. Chapman, H. Y. Toschka, F. M. Klis, and C. T. Verrips.** 1997. Comparison of cell wall proteins of *Saccharomyces cerevisiae* as anchors for cell surface expression of heterologous proteins. Appl. Environ. Microbiol. **63:**615–620.
133. **van Ulsen, P., L. van Alphen, J. ten Hove, F. Fransen, P. van der Ley, and J. Tommassen.** 2003. A neisserial autotransporter NalP modulating the processing of other autotransporters. Mol. Microbiol. **50:**1017–1030.
134. **Veiga, E., V. de Lorenzo, and L. A. Fernandez.** 2003. Autotransporters as scaffolds for novel bacterial adhesins: surface properties of *Escherichia coli* cells displaying Jun/Fos dimerization domains. J. Bacteriol. **185:**5585–5590.
135. **Veiga, E., V. De Lorenzo, and L. A. Fernandez.** 2003. Neutralization of enteric coronaviruses with *Escherichia coli* cells expressing single-chain Fv-autotransporter fusions. J. Virol. **77:**13396–13398.
136. **Veiga, E., V. de Lorenzo, and L. A. Fernandez.** 1999. Probing secretion and translocation of a beta-autotransporter using a reporter single-chain Fv as a cognate passenger domain. Mol. Microbiol. **33:**1232–1243.
137. **Veiga, E., V. de Lorenzo, and L. A. Fernandez.** 2004. Structural tolerance of bacterial autotransporters for folded passenger protein domains. Mol. Microbiol. **52:**1069–1080.
138. **Veiga, E., E. Sugawara, H. Nikaido, V. de Lorenzo, and L. A. Fernandez.** 2002. Export of autotransported proteins proceeds through an oligomeric ring shaped by C-terminal domains. EMBO J. **21:**2122–2131.
139. **Voulhoux, R., M. P. Bos, J. Geurtsen, M. Mols, and J. Tommassen.** 2003. Role of a highly conserved bacterial protein in outer membrane protein assembly. Science **299:**262–265.
140. **Voulhoux, R., and J. Tommassen.** 2004. Omp85, an evolutionarily conserved bacterial protein involved in outer-membrane-protein assembly. Res. Microbiol. **155:**129–135.
141. **Wentzel, A., A. Christmann, T. Adams, and H. Kolmar.** 2001. Display of passenger proteins on the surface of *Escherichia coli* K-12 by the enterohemorrhagic *E. coli* intimin EaeA. J. Bacteriol. **183:**7273–7284.
142. **Wentzel, A., A. Christmann, R. Kratzner, and H. Kolmar.** 1999. Sequence requirements of the GPNG beta-turn of the *Ecballium elaterium* trypsin inhibitor II explored by combinatorial library screening. J. Biol. Chem. **274:**21037–21043.
143. **Wernerus, H., and S. Stahl.** 2004. Biotechnological applications for surface-engineered bacteria. Biotechnol. Appl. Biochem. **40:**209–228.
144. **Wilhelm, S., J. Tommassen, and K. E. Jaeger.** 1999. A novel lipolytic enzyme located in the outer membrane of *Pseudomonas aeruginosa*. J. Bacteriol. **181:**6977–6986.

145. **Yanagida, N., T. Uozumi, and T. Beppu.** 1986. Specific excretion of *Serratia marcescens* protease through the outer membrane of *Escherichia coli*. J. Bacteriol. **166:**937–944.
146. **Yang, T. H., J. G. Pan, Y. S. Seo, and J. S. Rhee.** 2004. Use of *Pseudomonas putida* EstA as an anchoring motif for display of a periplasmic enzyme on the surface of *Escherichia coli*. Appl. Environ. Microbiol. **70:**6968–6976.
147. **Yavin, E. J., and M. Fridkin.** 1998. Peptides derived from human C-reactive protein inhibit the enzymatic activities of human leukocyte elastase and cathepsin G: use of overlapping peptide sequences to identify a unique inhibitor. J. Pept. Res. **51:**282–289.
148. **Yavin, E. J., L. Yan, D. M. Desiderio, and M. Fridkin.** 1996. Synthetic peptides derived from the sequence of human C-reactive protein inhibit the enzymatic activities of human leukocyte elastase and human leukocyte cathepsin G. Int. J. Pept. Protein Res. **48:**465–476.
149. **Yeung, Y. A., and K. D. Wittrup.** 2002. Quantitative screening of yeast surface-displayed polypeptide libraries by magnetic bead capture. Biotechnol. Prog. **18:**212–220.
150. **Zhu, C., F. Ruiz-Perez, Z. Yang, Y. Mao, V. L. Hackethal, K. M. Greco, W. Choy, K. Davis, J. R. Butterton, and E. C. Boedeker.** 2006. Delivery of heterologous protein antigens via hemolysin or autotransporter systems by an attenuated ler mutant of rabbit enteropathogenic *Escherichia coli*. Vaccine **24:**3821–3831.